

TU DELFT

Automatic classification of vault jumps using video analysis

Submitted by
Rick Oppedijk

Submitted
3/7/2013

Abstract

In sports, the use of motion-capture techniques increases, leading to a fast increase in valuable motion data. Automatic recognition and classification of the captured motions, provides an orderly structuring of the motion data. By this the users can easily retrieve specific motion data. In this thesis, we consider the automatic classification of vault jumps in gymnastics, captured by a high speed video camera system. A vault jump consists of a sequence of motions belonging to a predefined motion label, such as a Handspring. Then, the vault classification problem consists of automatically recognizing a vault jump in a video recording and assigning the appropriate label to the recording. To this end, we segment the vault classification problem into a sequence of vault-section classification problems. The following vault-sections are proposed; *Type of Vault (TV)*, *Number of Somersaults (NS)*, *Type of Somersault (TS)* and *Number of Twists (NT)*. The segmentation into vault-sections allows for the development of a versatile classification system, capable of classifying a large number of vault classes based on a limited amount of data. Next, we use video analysis techniques to transform a video recording into feature representations, or so called feature sets, which reflect the specific characteristics of the vault jump throughout the four vault-sections. The four vault-section feature sets are then classified, resulting in four vault-section classifications. The final labeling of the recording of a vault jump is by the combined results of the four vault-section classifications. The proposed automatic vault classification system is based on the vault jump recordings made by Van de Eb et al. [1] at the world championships in gymnastics 2010. Extensive experiments have been conducted on these recordings for evaluating various feature sets and classifiers per vault-section, resulting in one best performing combination per vault-section. Furthermore, the vault-section classifications are evaluated on their influence on the classification performance of a complete vault jump. In the end, an overall classification rate of 69.5%, with a correct classification accuracy of 90.2%, is obtained for the classification of the vault jump recordings.

1	Introduction	5
2	Vault Jumping.....	8
2.1	Description of a Vault Exercise	8
2.2	Physics in Vault Jumping	9
2.3	Manual Classification	10
3	Motion Classification	12
3.1	Automatic Classification Principle.....	12
3.2	Current Technologies	12
3.3	Video Analysis	13
3.4	Particle Measurements.....	13
4	Database Description	17
4.1	Vault-Sections	17
5	Vault Classification	20
5.1	Feature Generation.....	20
5.1.1	Regions of Interest	21
5.1.2	Physical Explanation.....	29
5.2	Feature Selection	31
5.2.1	Transformation Mappings.....	31
5.2.2	Reduced Feature Sets	32
5.3	Classifiers	35
6	Vault-section Evaluation	38
6.1	Evaluation Experiments	38
6.2	Vault-Section Results	40
6.2.1	Type of Vault (TV) Classification	40
6.2.2	Number of Somersaults (NS) Classification	40
6.2.3	Type of Somersault (TS) Classification	41
6.2.4	Number of Twists (NT) Classification	42
6.3	Conclusion.....	43
7	Classification Evaluation	44
7.1	Results Vault Classification	44
7.1.1	Combined Vault-Sections Evaluation.....	45
7.1.2	Segmentation Evaluation	46

7.2	Conclusion.....	47
8	Conclusion.....	48
9	Discussion.....	49
10	Recommendations	52
	Acknowledgements.....	53
	Appendix A.....	54
A.1	TV-50-50 Split Experiment Results.....	54
A.2	NS-50-50 Split Experiment Results.....	57
A.3	TS-50-50 Split Experiment Results	58
A.4	NT-50-50 Split Experiment Results	61
	Bibliography	66

1 Introduction

In sports, the use of motion-capturing techniques increases. Top athletes use motion-capture information to gain more knowledge about performed movements and to assess the execution of the movements. Also for gymnastics, new motion-capture techniques have been developed and applied. This leads to a fast increase in valuable motion data. Arranging these into an orderly structure has proven to be very labor intensive, especially for the recognition and classification of techniques. This has led to an increase in the development of automatic motion classification systems [2][3]. In general, a classification system assigns unclassified data to one of a given number of labels according to its contents. An automatic motion classification system maps an unknown motion data stream to a label according to the motion characteristics.

In this thesis, an automatic motion classification system for vault jumps in gymnastics will be developed. A vault jump consists of a sequence of motions belonging to a predefined motion label, such as a Handspring. Unlike some other gymnastic routines, vault jumping is performed within a confined space and only includes translations and rotations in two directions, namely twists and somersaults. This allows in principle for an optical motion-capture system, using a single camera, to capture the vault jumps. VU university Amsterdam, in collaboration with InnoSportLab 's-Hertogenbosch, developed a high speed video analysis system called the **TurnTrainersCockPit** (TTCP), to record and analyze gymnastic motions. The system is mainly used to capture motions performed on the Vault apparatus. The TTCP records and analyzes vault jumps in 2D and has been used at the world championships of artistic gymnastics 2010 in Rotterdam to record the vault jumps [1]. Furthermore, the TTCP is installed at the top Dutch gymnastics association Flik-Flak. The system is able to automatically record and analyze the vault jump characteristics, for example the flight path of the center of mass. It is however not capable of automatically classifying jumps into specific techniques, which would be a major timesaving addition to the system.

Automatic classification systems have already been applied in trampoline jumping [2]. Furthermore, they have extensively been implemented in human gait and activity researches [3][4][5]. Throughout the years a multitude of automatic classification methods have been developed [6]. Several comparative and empirical evaluation studies [4][7][8] have been performed and they all conclude that the optimal classification method depends on the problem at hand, thus an optimal classification method is not known beforehand. Automatic classification methods originate from the scientific fields of pattern recognition and statistics and they are mostly based on statistical methods known as supervised learning algorithms. In pattern recognition, the goal is to assign/classify objects, or patterns, into a number of classes/categories. Supervised learning algorithms make use of the fact that the true class labels are known in advance. This knowledge is used to train and test the classification method. The principles of a supervised learning algorithm are as followed. From an object, or pattern, a set of numerical measures, known as features, is extracted by a preprocessor. This feature set is then presented to a classifier which maps the feature set to a class. The classifier is trained and tested by comparing the predicted class with the true class of the object/pattern. A well respected book in the pattern recognition world is the book "Pattern Recognition", by Theodoridis et al. [9]. In this book they propose the following design stages for designing an automatic classification procedure: sensor, feature generation, feature selection,

classifier design and system evaluation. Figure 1.1 shows a schematic representation of the design sequence.

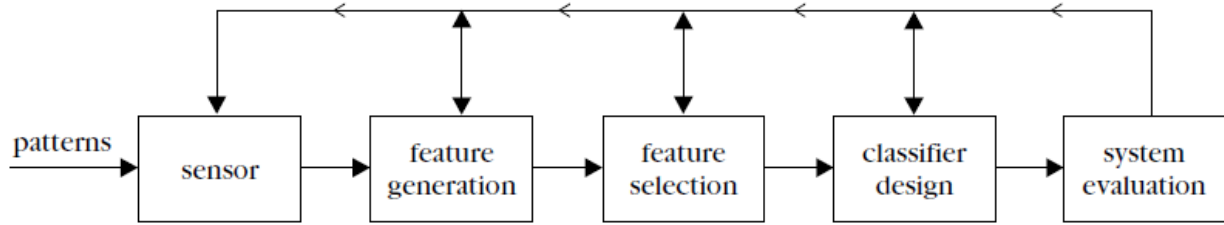


Figure 1.1 Basic stages for designing a classification system. Figure is from the book "Pattern Recognition" by Theodoridis et al. [9].

The classification problem of this thesis comprises the automatic assignment of vault jump recordings, made by the TTCP, to the corresponding motion labels with a sufficient accuracy. The automatic vault classification system is designed in a similar manner as the design stages proposed by Theodoridis et al. [9]. The classification procedure of this thesis consists of a preprocessor, classifier and evaluation method and will be based on the recordings database of the world championships of artistic gymnastics 2010. In addition to the design of the classification procedure, a segmentation methodology will be proposed, expanding the diversity of the classification system. The classification system will contain jump classes from different vault types, and jump classes that are in a biophysical way much alike.

The Code of Points, which is the rulebook by the international gymnastics federation FIG, contains 104 different jumps. The ideal classification method to classify vault jumps must ideally be able to classify all jumps. Furthermore, the system must be robust against inter-performance variations, where the same jump is performed by different gymnasts, and intra-performance variations where a jump is performed multiple times by the same gymnast. Such a system also needs to be sensitive enough to make the distinction between jumps that are much alike. To guarantee that the optimal classification method is used, a multiple of preprocessors and classifiers, ranging from simple linear to complex nonlinear classifiers, will be designed and evaluated using the same database. The design of the preprocessors and classifiers will be based on the principles of supervised learning.

This thesis is structured as follows. In Chapter 2, an introduction to vault jumping is given, including a detailed description of a vault exercise, the physics involved in vault jumping and a description of the manual classification. Chapter 3 gives a general introduction into the motion classification task of this thesis. The necessary elements of a motion classification system, like the database, preprocessor and classifier, are introduced. Furthermore, a summary of the current technologies in motion classification and a detailed explanation of the TTCP video analysis system is given, including the numerical measurements representing the motions. In Chapter 4, a detailed description of the database is given. Furthermore, a segmentation methodology is proposed. Segmenting the classification problem into a sequence of classification problems, allows for a diverse classification system and an optimal use of the database. Chapter 5 gives a detailed explanation of the automatic vault classification system. For each vault-section, proposed in Chapter 4, different feature sets are described. Algorithms for optimizing the feature sets are introduced and described. Also the classifiers used in this thesis are described. Chapters

6 and 7 contain the evaluation experiments performed in this thesis. Chapter 6 evaluates the feature sets, classifiers and rejection types proposed in Chapter 5. The evaluation is done for every vault-section individually and will result in an optimal feature set - classifier - rejection combination for each vault-section. Chapter 7 validates the vault classification system using the chosen feature sets from Chapter 6. The validation is done for the classification of a complete vault jump. In Chapter 8 we present the main conclusions of this thesis. In addition to the conclusions of Chapter 8, we will hold a discussion on the classification performances in Chapter 9. Chapter 10 ends this thesis by giving recommendations for future work.

2 Vault Jumping

The motion classification system proposed in this thesis is developed for the gymnastics routine known as **Vault Jumping**, where athletes perform acrobatic moves while vaulting over the vault table. Gymnastics originates back to the ancient Olympic Games and is one of the oldest Olympic sports. Gymnastics, and vault jumping, is being performed at every Olympic games of the modern era starting from 1896 [10].

Vault jumping includes complex dynamical movements like somersaults and twists (Figure 2.1). To better understand which specific motion characteristics separate one jump from the others, a general knowledge about the motions involved in vault jumping is helpful. In this chapter a description of a vault exercise is given in section 2.1. In section 2.2, an insight in the physics involved in gymnastics is given, with reference to previously applied studies. The vault labels by the FIG Code of Points are introduced in section 2.3.

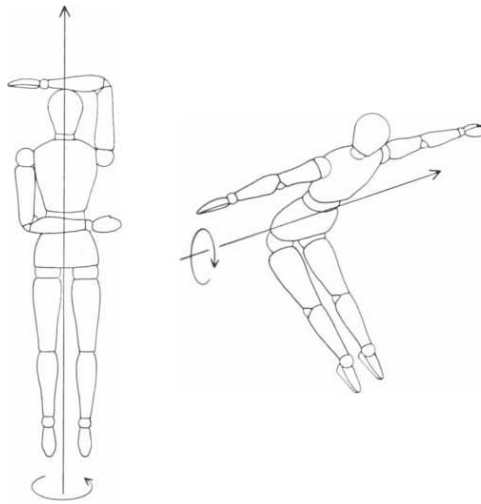


Figure 2.1 Axes of rotation for twists (left) and somersaults (right). Figure is from [11].

2.1 Description of a Vault Exercise

The vault apparatus is included both in mens and womens gymnastics. A vault jump starts at the beginning of a 25 meter runway, which leads to the vaulting board and the vaulting table, and ends behind the vaulting table. A vault jump is defined by the sequence of motions performed in the following time sections: the *approach*, *first flight phase* and the *second flight phase*. For a good understanding of the physics and dynamics involved in a vault routine, each section will be addressed briefly.

The approach: The approach starts at the beginning of the runway and ends at the vaulting board. The approach consists of the run-up towards the vaulting board and the preparation before take-off from the vaulting board. In the preparation phase, the gymnast may perform a hurdle step on the vaulting board, resulting in a front-ways take-off, or a round-off (Figure 2.2), resulting in a backwards take-off.

First flight phase: The first flight phase is initiated by the take-off from the vaulting board and ends when the gymnast hits the vaulting table. It is obligatory to hit the vaulting table only by hands. The gymnast is allowed to perform a quarter, half or a full twist (90° , 180° or 360°) but is not allowed to perform any kind of somersaults in the first flight phase.

Second flight phase: The second flight phase is initiated by the push-off from the vaulting table. In the second flight phase, the gymnast is allowed to perform a number of twists and somersaults while maintaining a certain body posture, see Figure 2.3 for the different body postures. Vaults with straddled legs are not permitted. The second flight phase ends with a landing on the mat behind the vaulting board. The landing must result in a standing position with the legs together. The gymnast must be facing towards, or away from, the vaulting table. This concludes the vault jump.



Figure 2.2 Round-off entry resulting in a backwards take-off from the vaulting board. Figure is from [12].



Figure 2.3 Body postures, from left to right: Tucked, Piked, Layout. Figure is from [12].

2.2 Physics in Vault Jumping

Several scientific studies have been performed to gain more insight in the kinematics of gymnastics, in specific vault jumping. Van der Eb et al. [1] analyzed high-speed video recordings of male and female gymnasts, recorded at the Rotterdam Artistic Gymnastics World Championships 2010. They showed that a vault routine has specific kinematic characteristics. During the run-up, male gymnasts accelerated to maximum velocities up to $8.4 \pm 0.3 \text{ m} \cdot \text{s}^{-1}$. At the point of last foot contact to the runway, male gymnasts still have a velocity of $8.2 \pm 0.5 \text{ m} \cdot \text{s}^{-1}$ (these results are for Handspring type of vaults). For Tsukahara and Yurchenko type of vaults (see section 2.3 for details of these vaults) the maximum velocities are respectively 8.2 ± 0.4 and $7.7 \pm 0.3 \text{ m} \cdot \text{s}^{-1}$ and the velocities at the point of last foot contact are 8.0 ± 0.6 and $6.6 \pm 0.7 \text{ m} \cdot \text{s}^{-1}$.

Previous studies also showed that the flight trajectory of the gymnast is not only determined by the take-off from the vaulting board but also by the push-off from the vaulting table. The vaulting board is used to direct the mainly horizontal run-up speed into a combination of horizontal and vertical speed,






needed to clear the vaulting table and to gain enough flight time for executing somersaults and twists. The adjusting of the gymnasts momentum direction, by the take-off and push-off, is accompanied with high forces and thus accelerations. Yeadon et al. [13] created a physical two-segment model of a gymnast to investigate the reversal of rotation in a Hecht-vault (where the direction of the somersault rotation is reversed during contact with the vaulting table). By initiating the model with realistic take-off conditions from the vaulting board, they discovered that over half of the reversal rate is due to the flight trajectory in the first flight phase. We must note that currently Hecht vaults are no longer included in vault jumping, see [12]

The execution of somersaults and twists in midair is made possible by the law of conservation of angular momentum. Cliff Frohlich et al. [11] stated that angular momentum consists of two parameters, angular velocity and moment of inertia, and that the total angular momentum is constant in midair. By changing their body posture in midair, a gymnast changes his moment of inertia and thus changes his angular speed, which allows him to perform somersaults and twists.

2.3 Manual Classification

The manual classification task comprises the manual labeling of the motions, based on the rulebook known as the Code of Points. For male and female gymnastics different codes of points exist [12][14]. All the jumps included in the code of points for women are also included in the code of points for men, which consists of 104 different vault classes. The jump labels included in the vault classification system are according to the code of points for men. A vault is labeled by the type of vault (see Table 2.1), the number of performed rotations during the second flight phase and body posture during the second flight phase.

Table 2.1 Description of the five vault types.

Vault Type	Description	Schematic representation
Handspring/Yamashita	Hurdle entry, Frontward take-off	
Tsukahara/Kasamatsu	Hurdle entry, Frontward take-off, $\frac{1}{4}$ or $\frac{1}{2}$ turn in the 1 st flight phase	
Yurchenko	Round-off entry, backward take-off	
Yurchenko $\frac{1}{2}$	Round-off entry, backward take-off, $\frac{1}{2}$ turn in the 1 st flight phase	
Yurchenko 1/1	Round-off entry, backward take-off, 1/1 turn in the 1 st flight phase	

3 Motion Classification

The development of an automatic motion classification system includes three methodologies: the performance of motions, the capturing of motions and the analysis of motion-capture data. For this thesis, this concerns the performance of vault jumps, the capturing by high-speed video cameras and the analysis of the recordings. An extensive description of a vault jump was given in chapter 2. In this chapter the capturing of motions and a first step into the analysis of motion-capture data is given. First, an introduction to the terminology and principles of automatic classification is given in section 3.1 and a summary of the current technologies in motion classification is given in section 3.2. Subsequently, a description of the vault motion-capture system “TurnTrainersCockPit” is given in section 3.3 and a detailed description of the first analysis step is given in section 3.4.

3.1 Automatic Classification Principle

The automatic vault classification procedure is based on algorithms originating from the field of pattern recognition and statistics. Let us introduce the pattern recognition terminology and principles, where the terminology is the same as in the book "Pattern Recognition" by Theodoridis et al. [9]). Objects, in our case vault jump motion data, are known as *patterns*. A pattern belongs to a *class* and the name of the class is known as a *label*. From a pattern, different *features* can be extracted, this is called *feature generation*. A feature is a numerical measure of the pattern, thus a pattern is numerically represented by a *feature set*. It is up to the designer to select the features that represent the pattern the best. This is done by *feature selection*. Features are the input to the classification algorithm, known as the *classifier*. The classifier is the algorithm that maps the input, feature set, to the output, class-label. *Training patterns* are feature sets that are used for training the classifier. The training patterns are presented to the classifier with their accompanying true-labels. *Test patterns* are used to evaluate the performance of the classifier and are presented to the classifiers as unknown patterns. Test patterns assigned to a class-label different from the true-label are called *misclassified*. A test pattern can be correctly classified, misclassified or rejected.

3.2 Current Technologies

Motion-capture data are increasingly used as input for automatic motion classification systems. Especially inertial sensor data and video analysis serve as input to motion classification systems [15][4]. Image classification methods generally focus on initialization, tracking, pose estimation, and movement recognition [16]. The movement recognition methods are mostly used for the analysis of gait parameters and identification of human movements.

The application of automatic classification systems in gymnastics has currently not been investigated. However, Brock et al. [17] developed an automatic classification system for capturing, segmenting, and classifying trampoline routines. They used inertial sensors to capture the trampoline jumps. From the inertial sensor data they extracted a multitude of feature vectors. As feature selection method they used a variant of dynamic time warping and dynamic programming to generate motion templates. The classification is based on comparative measures (Euclidian L^2 norm) and the evaluation is done by confusion matrices. They obtained a classification rate of 84.65%.

Troje [5] developed a framework that allows for gender recognition from gait data, using a linear classifier. They used Principal component analysis as feature selection method and revealed that the best classification only includes 4 components and resulted in a classification error of 7.5% (3 out of 40 samples misclassified). Their proposed artificial gender classification procedure performed better than human observers, who received the same motion information via a point-light display. The artificial gender recognition procedure reflected a similar behavior as human vision recognition. This demonstrates that by designing an automatic motion classification system, also a deeper knowledge about the motions is obtained.

3.3 Video Analysis

Nowadays many different techniques exist to capture motions. Optical systems are by far the most commonly used, but also inertial, mechanical and magnetic sensor systems exist. The applicability of motion-capturing techniques is usually expressed in several properties concerning the recording environment, capturing volume and mobility. Considering the capturing of vault jumps in gymnastics, the mobility of the gymnast is of utmost importance. The motion-capturing technique may not restrict the mobility of the gymnast in any way. Given this requirement, optical markerless systems are most suitable for capturing vault jumps. Optical markerless systems are noninvasive to the gymnast and their capturing volume is large enough to capture vault jumps, as is done by Van der Eb et al. [1].

Optical markerless systems generally use high-speed video cameras to capture the highly dynamical motions. A single camera provides 2D information about the motion. A setup with multiple cameras is able to capture full 3D information. For a good performance of optical markerless systems, the environmental conditions are of utmost importance, especially concerning the lighting conditions and the background. Furthermore, extensive calibration of the system is needed. A disadvantage of optical systems is the large overhead in setting up and calibrating the system. For the application of automatic vault classification, the video images also need extensive preprocessing, to segment the motion of the gymnast from its surroundings. Another weakness of optical markerless motion capturing systems is that the recorded motions are not bound to one single moving object, thus objects moving in the background are also observed, which will induce errors.

The optical markerless high-speed video analysis tool “TurnTrainersCockPit” (TTCP) is developed by the VU Amsterdam for the analysis of gymnastic motions, specifically vault jumping. At the world championships artistic gymnastics 2010, the TTCP was used to record the vault jumps made during competition. The camera recorded the motions in the sagittal plane, with a sample frequency of 100 Hz. A standard direct 2D linear transformation method was used to calibrate the camera.

3.4 Particle Measurements

After a vault jump is captured by the TTCP, it is analyzed to segment the dynamical motions of the gymnast from the static background. From the segmented image, numerical measures are extracted that represent the motion characteristics. These numerical measures are the pattern of the vault jump.

To generate the segmented image and vault patterns an image analysis technique known as **Particle Analysis** is used [18]. Particle analysis consists of locating groupings of connected nonzero pixels, known

as *particles*, within an image, and applying measurements, known as *Particle Measurements*, on these particles. First a threshold is used to generate a binary image, where the pixels that belong to the background are set to zero and the rest (foreground) is given a value of 1. The TTCP uses a low-pass background filter as threshold. After thresholding, binary morphological operations are applied. Binary morphological operations extract and alter the structure of the particle to remove discontinuities within the particle. By this the gymnast is represented by a single particle, see Figure 3.1. The combination of the thresholding and morphological operations can be seen as a function $f(x, y)$, which defines whether pixel p_k , of frame k with coordinates (x_p, y_p) , belongs to the particle or not. From the binary image, particle measurements are extracted. In total 26 particle measurements are extracted. However, not every particle measure has proven to contain characteristic motion information, useful for automatic classification. For the automatic classification of vault jumps, the following particle measurements have proven to obtain motion characteristics: *Orientation*, *Area*, *Hu Moment 1*, *Rotated Bounding Rectangle Length 1*, *Rotated Bounding Rectangle Length 2*. Table 3.2 gives an overview of the particle measurements, the definition is by [18]. The sums are short hand notations, see Table 3.1 for the full notations of the sums. Note that Table 3.2 also includes the particle measurement X_{CoM} . This particle measurement is used for visualization of the motion characteristics in chapter 5. In addition to Table 3.2, a detailed description of the Orientation, Rotated Bounding Rectangle and the Hu Moment 1 will be given below.

Orientation: the Orientation (\emptyset) of the particle is defined as the angle between the line with the lowest moment of inertia that passes through the Center of Mass and the x-axis, where a counterclockwise rotation is considered positive. In Figure 3.2 the orientation is indicated by the magenta line. \emptyset is given in degrees and is mapped into the range of $0^\circ - 180^\circ$. Due to the tangent used to calculate \emptyset , rotations exceeding 180° are also mapped into the range of $0^\circ - 180^\circ$. This causes a discontinuous signal and the TTCP corrects for this by subtracting 180° each time a discontinuity occurs.

Rotated Bounding Rectangle: the Rotated Bounding Rectangle (*RBR*) is defined as the smallest rectangle that encloses the particle completely, where the orientation of the rectangle is equal to \emptyset , see Figure 3.2. The length of the *RBR* is called the Rotating Bounding Rectangle Length 1. The width is referred to as the Rotating Bounding Rectangle Length 2. Units are in pixels.

Hu Moment 1: the Hu Moment 1 (Hu_1) is the sum of the normalized moments of inertia about the x and y axis. The sum of two moments of inertia about two principle axes equals the moment of inertia about the third principle axis, thus the Hu Moment 1 represents the normalized moment of inertia about the local z-axis, which is perpendicular to the image. The Hu Moment 1 is rotational and space invariant. Furthermore, the Hu Moment 1 is size invariant.

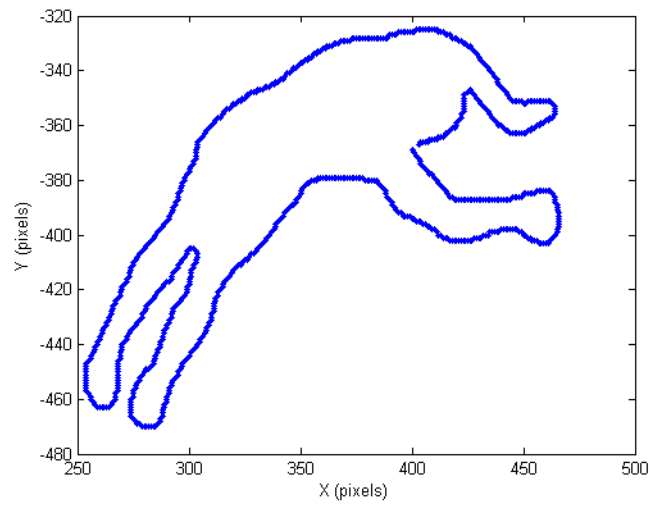


Figure 3.1 Binary image after the application of thresholding and binary morphology operations.

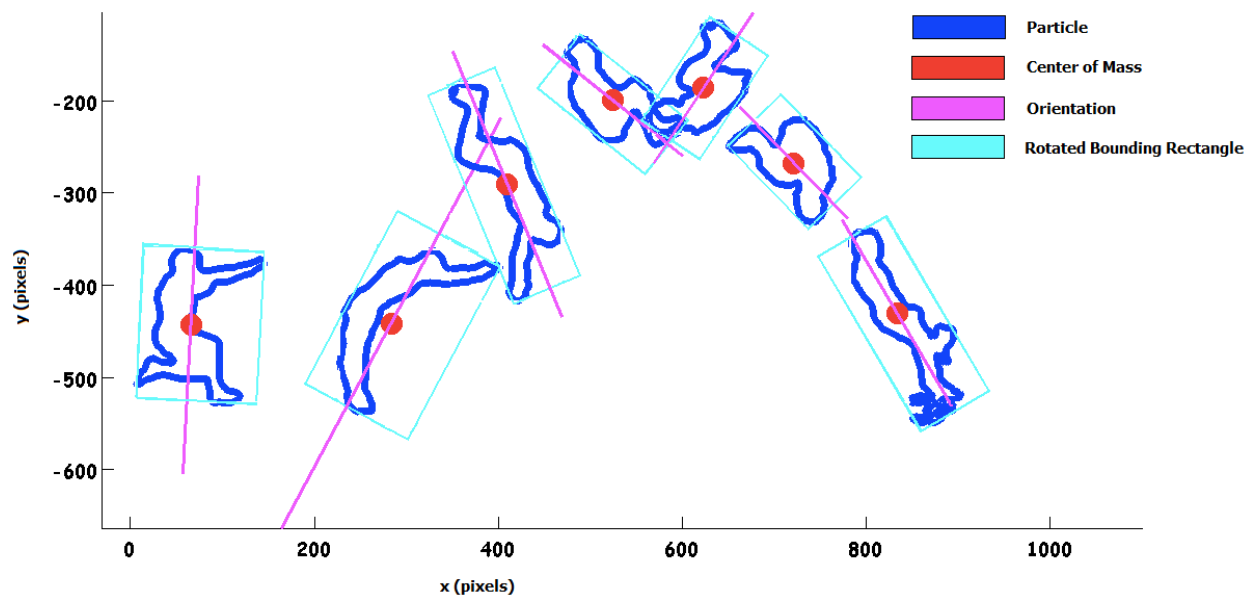


Figure 3.2 Schematic representation of the particle measurements.

Table 3.1 Full notations of the sums used in Table 3.2.

Short hand notation	Full notation
\sum	$\sum_{x=1}^i \sum_{y=1}^j$
$\sum(x)$	$\sum_{x=1}^i \sum_{y=1}^j (x \cdot f(x, y))$
$\sum(y)$	$\sum_{x=1}^i \sum_{y=1}^j (y \cdot f(x, y))$
$\sum(xx)$	$\sum_{x=1}^i \sum_{y=1}^j (x \cdot x \cdot f(x, y))$
$\sum(xy)$	$\sum_{x=1}^i \sum_{y=1}^j (x \cdot y \cdot f(x, y))$
$\sum(yy)$	$\sum_{x=1}^i \sum_{y=1}^j (y \cdot y \cdot f(x, y))$

Table 3.2 Overview of the Particle Measurements used in this thesis.

Particle Measurement	Definition	Symbol	Equation
Area	Area of the particle	A	$\sum f(x, y)$
Center of Mass x	X-coordinate of the particle Center of Mass	X_{CoM}	$\frac{\sum(x)}{A}$
Orientation	The angle of the line that passes through the particle Center of Mass about which the particle has the lowest moment of inertia	\emptyset	$\frac{1}{2} \text{atan} \left(\frac{2 \sum(xy)}{\sum(yy) - \sum(xx)} \right)$
Moment of Inertia xx	Moment of Inertia around the y-axis	I_{xx}	$\sum(xx) - \frac{\sum(x) \cdot \sum(x)}{A}$
Moment of Inertia yy	Moment of Inertia around the x-axis	I_{yy}	$\sum(yy) - \frac{\sum(y) \cdot \sum(y)}{A}$
Norm. Moment of Inertia xx	Normalized Moment of Inertia around the y-axis	N_{xx}	$\frac{I_{xx}}{A^2}$
Norm. Moment of Inertia yy	Normalized Moment of Inertia around the x-axis	N_{yy}	$\frac{I_{yy}}{A^2}$
Hu Moment 1	Sum of the Normalized Moments of Inertia	Hu_1	$N_{xx} + N_{yy}$
Rotated Bounding Rect Left	X-coordinate of the leftmost rotated particle point	RBR_L	
Rotated Bounding Rect Top	Y-coordinate of the highest rotated particle point	RBR_T	
Rotated Bounding Rect Right	X-coordinate of the rightmost rotated particle point	RBR_R	
Rotated Bounding Rect Bottom	Y-coordinate of the lowest rotated particle point	RBR_B	
Rotated Bounding Rect Length 1	Length of the rotated bounding rectangle	$RBR1$	$RBR_T - RBR_B$
Rotated Bounding Rect Length 2	Width of the rotated bounding rectangle	$RBR2$	$RBR_R - RBR_L$

4 Database Description

The automatic vault classification system is based on the Rotterdam Artistic Gymnastics World Championships 2010 database (WC 2010). Although the classification system should be complete not all the 104 vault classes from the FIG Code of Points are included in the database. Furthermore, the amount of data is limited and not every class is presented by 10 or more samples. In this chapter a segmentation methodology is described, that in principle allows for classifying a higher number of vault classes than the number of vault classes included in the WC 2010. In theory, the segmentation even allows for the classification of vault jumps not included in the FIG Code of Points, for example a Handspring with a double layout somersault and a double twist.

In section 4.1, the WC 2010 database is described. Furthermore, the segmentation of the database into vault-sections is proposed. It is described how segmentation of a vault class into vault-section classes allows for a more divers classification system.

4.1 Vault-Sections

The database of the Rotterdam Artistic Gymnastics World Championships 2010 consists of 618 vaults (341 male, 277 female). The database contains 151 Handspring (81 male, 70 female), 225 Tsukahara (203 male, 22 female), 219 Yurchenko (53 male, 166 female) and 23 Yurchenko 1/2 (4 male, 19 female) types of vaults. No jumps were performed containing a Yurchenko 1/1 type of vault. See the figures from Table 2.1 for a schematic representation of the vault types. The database contains vaults from 45 different classes, where 18 classes contain samples from solely female gymnasts, 14 classes contain samples from solely male gymnasts and 13 classes contain samples from both male and female gymnasts. The number of samples per class varies widely, from only 1 sample up to 82 samples. For a somewhat reliable classification, at least 10 samples are needed from each class. Applying this rule of thumb leaves only 17 classes, which covers 86.7% of the data (536 jumps), see Table 4.1. Furthermore, Yurchenko 1/2 type of vaults are not included in Table 4.1. The most obvious solution for this problem would be to enlarge the database such that every class contains 10 or more samples. However this proves to be a rather challenging and cumbersome approach. Furthermore, viewing each vault class as completely independent would be naïve, because some classes are much alike and only differ, for example, by half a twist.

Instead of viewing the vaults as one time series, a vault jump can also be represented as a sequence, or combination, of motions, by segmenting the vault into sections. The segmentation allows the defining of *section-classes*, where the number of classes per section is lower than the number of original FIG Code of Points classes. The combination of the section classes matches the vault classes. By segmenting, the amount of samples per section class is increased, thus more combinations of section classes can be made. This results in a classification method capable of classifying a higher degree of FIG Code of Points classes. A drawback of the segmentation is that it considers each vault-section to be independent, thus possible relations between sections are neglected.

Table 4.1 Table of vault classes containing more than 10 samples.

Performed by	Type of vault	Somersaults	Type of somersault	Twists	Samples
Male and Female	Handspring	1	Tucked	0	24
		1	Layout	1.5	19
	Tsukahara	1	Layout	1	57
		1	Layout	2	68
	Yurchenko	1	Layout	0	19
		1	Layout	1	66
		1	Layout	1.5	26
		1	Layout	2	82
		1	Layout	2.5	19
Male	Handspring	2	Tucked	0	34
		2	Tucked	0.5	13
	Tsukahara	1	Layout	1.5	15
		1	Layout	2.5	46
Female	Handspring	2	Piked	0	10
		1	Piked	0.5	12
	Tsukahara	1	Piked	0	14
		1	Piked	0	12
TOTAL:	17/45 vault classes				536

The segmentation methodology consists of two segmentation parts. The first part comprises the segmentation of vault labels into vault-section labels. The second part comprises the segmentation of vault patterns (particle measurements) into vault-section feature sets, this corresponds with the feature generation design stage proposed by Theodoridis et al. The feature generation stage will be discussed in chapter 5.

The segmentation of the vault labels into vault-section labels is done parallel to the reasoning used to manually classify a vault jump, namely, what type of vault is performed, how many somersaults are performed, what is the body posture during the somersaults and how many twists are performed, resulting in the following vault-sections: *Type of Vault*, *Number of Somersaults*, *Type of Somersault* and *Number of Twists*. In Table 4.2 the classes per vault-section, with the accompanying amount of samples, is given. Table 4.2 shows that for each vault-section the full set of 618 samples is used and that almost all the vault-section classes include more than 10 samples, except for the classes "0 somersaults" and "3 twists". This is due to the fact that vaults including 0 somersaults are too easy for a world championships event, and that vaults including 3 twists are extremely difficult and can only be performed by a view top athletes.

Table 4.2 Table of vault-section classes.

Section	Classes	Samples
Type of Vault	Handspring Tsukahara Yurchenko Yurchenko 1/2	151 225 219 23
Number of Somersaults	0 1 2	1 559 58
Type of Somersault	Tucked Piked Layout	87 62 469
Number of Twists	0 0.5 1 1.5 2 2.5 3	132 50 135 63 158 72 8

5 Vault Classification

The first step within the analysis of the motion-capture data, consisting of generating numerical measures of the high-speed video recordings, was discussed in section 3.4, resulting in the vault patterns. In this chapter, the analysis of motion-capture data is completed, wrapping up the design of the automatic vault classification system. This involves the following design steps: *Feature Generation*, *Feature Selection* and *Classifier Design*.

In section 5.1, the second step of the segmentation methodology, proposed in section 4.1, is performed. For each vault-section, different regions of interest within the particle measurements are selected, resulting in specific feature matrices for each vault-section. For a good performance of the classification procedure, a feature matrix must contain a high discriminative power, meaning that each feature represents different jump characteristics and optimizes the separation between the section classes. Furthermore, in section 5.1, a physical explanation of the jump characteristics is given. Section 5.2 covers the feature selection design stage. The feature matrices proposed in section 5.1 are reduced by applying transformation mappings. Several transformation mappings are proposed to reduce the feature matrices to optimized feature sets. The Dynamic Time Warping transformation mapping is treated with special interest. The proposed algorithm is similar to the dynamic time warping algorithm used in the automatic classification system for trampoline jumps, by Brock et al. [17]. In section 5.3, a variety of classifiers is proposed. The proposed classifiers are all included in the Matlab PRTTools toolbox, developed by The Pattern Recognition Research Group of the TU Delft [19], except for the classifier based on the Dynamic Time Warping mapping.

5.1 Feature Generation

The second step of the segmentation methodology involves the segmentation of vault patterns into vault-section feature matrices. This involves selecting different particle measurements to represent the vault-sections. However, the particle measurements do not have a high discriminative power over all the vault-sections. Therefore, we investigate the particle measurement data to find trends in the data that separate one class from the others. These trends are known as *regions of interest*. By this, each vault-section is represented by a feature matrix $X \in \mathbb{R}^{M \times P}$ (equation 5.1), where M depicts the number of selected particle measurements and P is the number of section frames.

$$X = \begin{pmatrix} x_{1,1} & \cdots & x_{1,P} \\ \vdots & \ddots & \vdots \\ x_{M,1} & \cdots & x_{M,P} \end{pmatrix} \in \mathbb{R}^{M \times P} \quad (5.1)$$

As stated in section 2.1, the Type of Vault vault-section is defined by the motions performed in the preparation and first flight phase. The other vault-sections all occur in the second flight phase. Therefore, the particle measurements are firstly split between the first flight phase and the second flight phase. The split is made at the frame containing the last hand contact to the vaulting table, from here on referred to as point of last hand contact. Furthermore, the second flight phase ends at the landing, thus the particle measurements are cut off at the moment of first contact with the landing mat. The frames containing the point of last hand contact and the first contact with the landing mat are automatically detected by the TTCP.

5.1.1 Regions of Interest

For locating the regions of interest, a visual inspection of the particle measurements is performed. The visual inspection consists of plotting, for all the section class samples, the particle measurements versus the x-coordinate of the Center of Mass (X_{CoM}). To align all the samples in space, we normalize X_{CoM} to $[-1,1]$, for each vault-section.

Type of Vault:

For the type of vault we only consider data occurring in the preparation and first flight phase, depicted by the lowercase index FFP. After investigating the particle measurement data we locate regions of interest within the Orientation particle measurement (ϕ_{FFP}) and the Area particle measurement (A_{FFP}). Let us first consider ϕ_{FFP} .

Figure 5.1 shows, for all the samples of the four Type of Vault classes, ϕ_{FFP} versus $X_{CoM_{FFP}}$. Figure 5.1 shows a clear distinction between Yurchenko and Yurchenko 1/2 type of vaults versus Handspring and Tsukahara type of vaults. The Yurchenko and Yurchenko 1/2 type of vaults show a clear linear trend that can easily be approximated by a first order polynomial. The Handspring and Tsukahara type of vaults, on the other hand, show a trend that can be approximated by a combination of linear fits. Furthermore, notice that the Yurchenko and Yurchenko 1/2 type of vaults perceive a rotation of approximately -400° , while the Handspring and Tsukahara type of vaults perceive a rotation of approximately -200° . Although, the perceived orientation values contain a high discriminative power, Figure 5.1 also shows a large inner-class variation. Normalizing ϕ_{FFP} to $[-1,1]$, resolves the inner-class variation while maintaining the motion characteristic shapes. However, the absolute values of the perceived orientation are lost, see Figure 5.2.

Figure 5.1 and Figure 5.2 both show a clear distinction between Yurchenko and Yurchenko $\frac{1}{2}$ versus Handspring and Tsukahara type of vaults. However, the distinction between Yurchenko or Yurchenko 1/2 type of vaults, and Handspring or Tsukahara type of vaults, is far less clear.

Next we consider the A_{FFP} . Figure 5.3 shows A_{FFP} versus $X_{CoM_{FFP}}$. Figure 5.3 shows that the trends for the Handspring and Tsukahara type of vaults slightly differ. However, a high interclass variation is present. Figure 5.4 shows that we magnify the trends by normalizing A_{FFP} to $[-1,1]$. Furthermore, it shows that A_{FFP} of the Handspring and Yurchenko type of vault drops between $X_{CoM_{FFP}} = 0$ and $X_{CoM_{FFP}} = 0.8$. The Tsukahara and Yurchenko $\frac{1}{2}$ type of vaults do not show this dip.

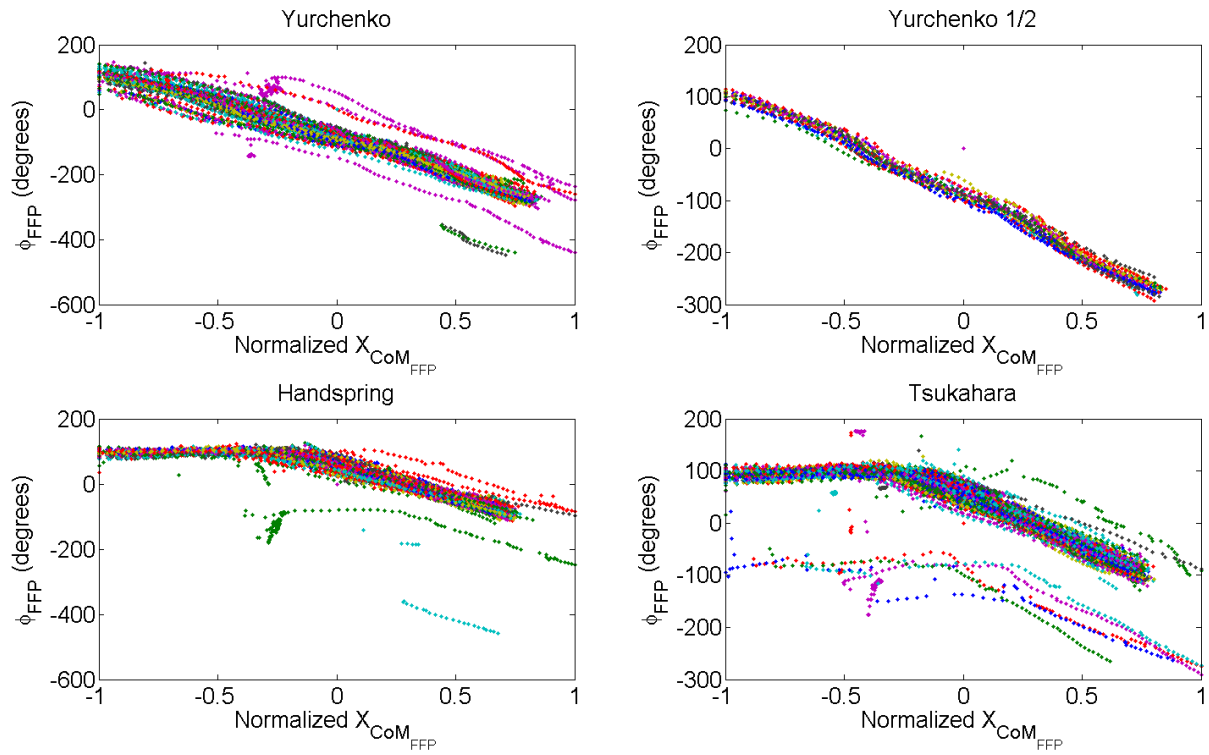


Figure 5.1 Normalized $X_{CoM_{FFP}}$ vs ϕ_{FFP} for the four Type of Vault classes.

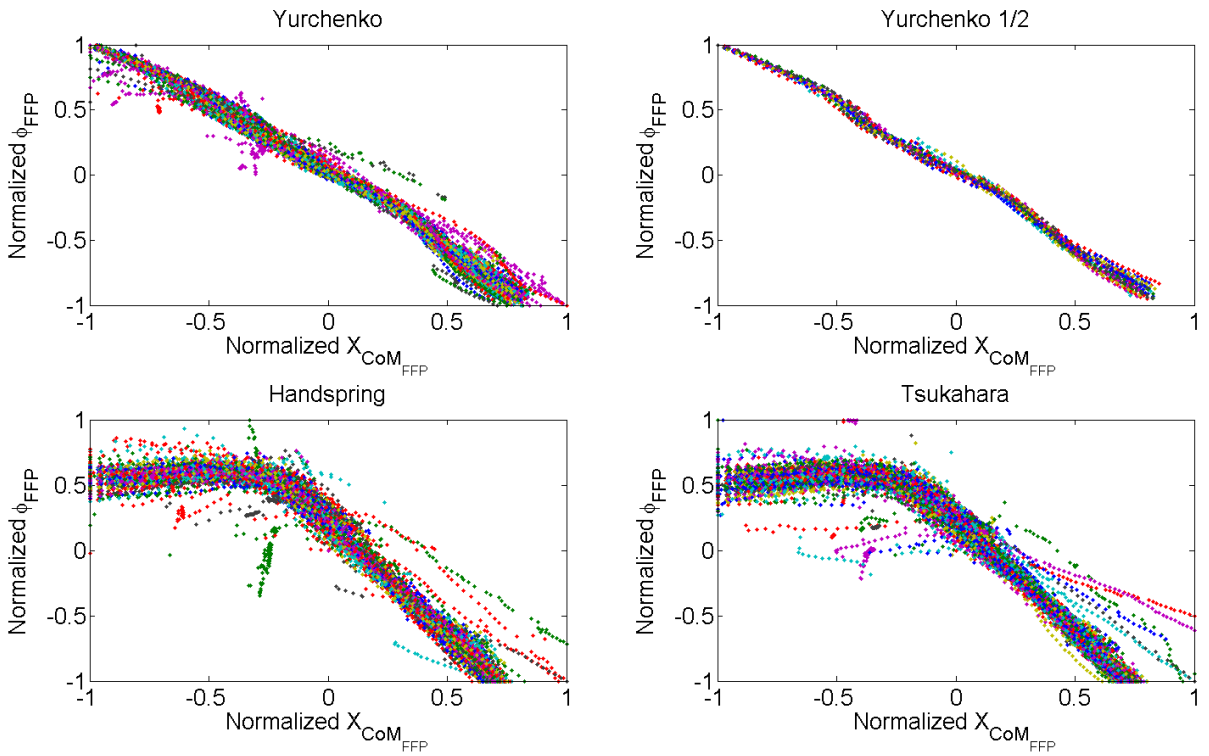


Figure 5.2 Normalized $X_{CoM_{FFP}}$ vs normalized ϕ_{FFP} for the four Type of Vault classes.

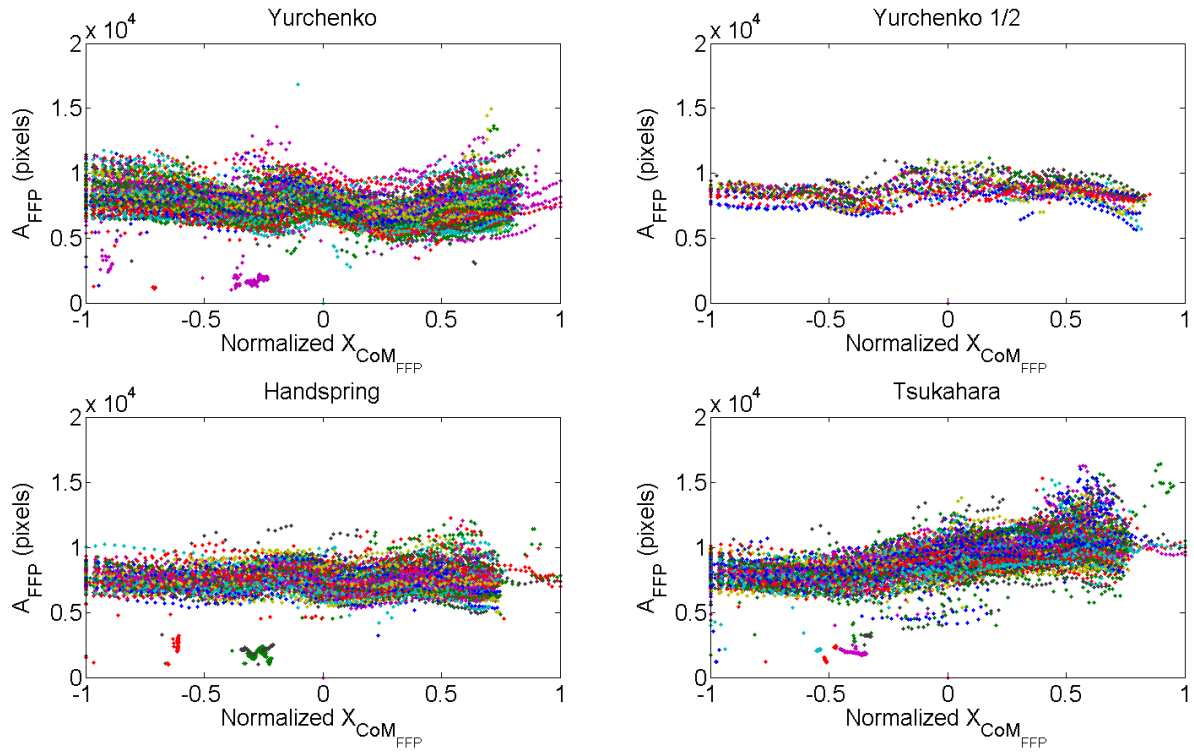


Figure 5.3 Normalized $X_{CoM_{FFP}}$ vs A_{FFP} for the four Type of Vault classes.

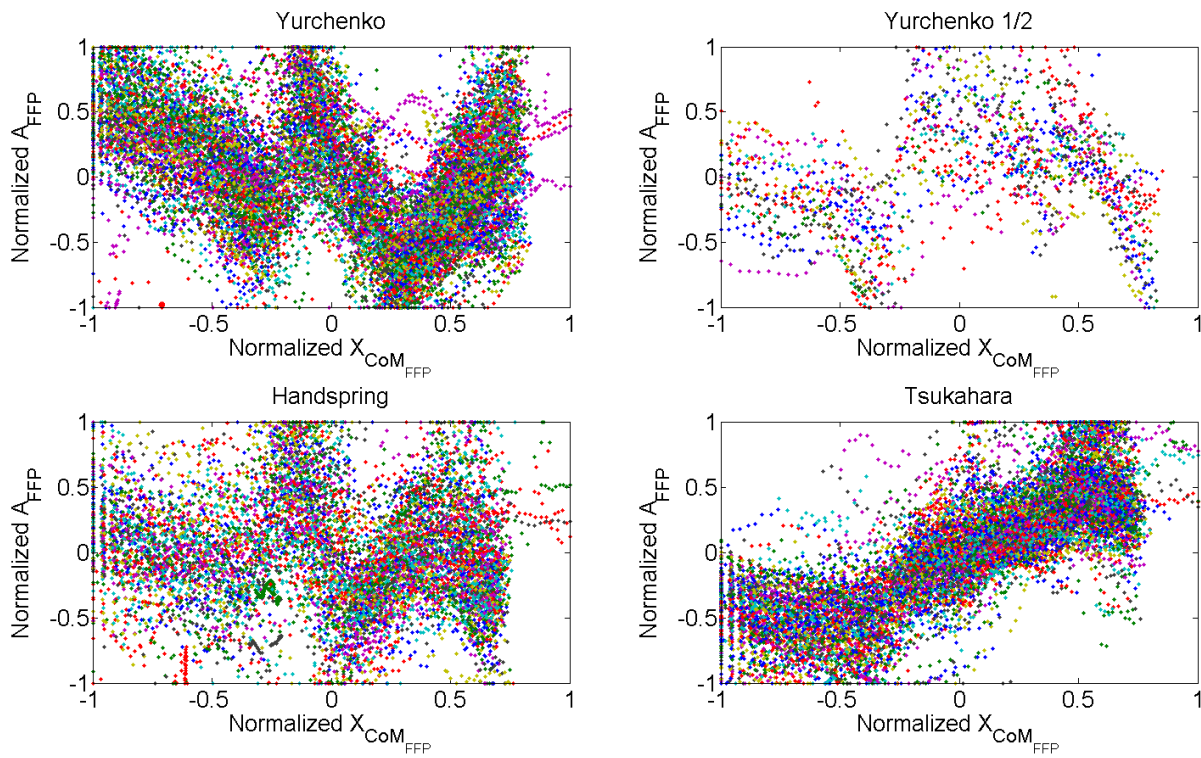


Figure 5.4 Normalized $X_{CoM_{FFP}}$ vs normalized A_{FFP} for the four Type of Vault classes.

Number of Somersaults:

For the Number of Somersaults section we only consider data occurring in the second flight phase, depicted by the lowercase index SFP. After investigating the particle measurements we locate regions of interest within the Orientation particle measurement (ϕ_{SFP}). Figure 5.5 shows ϕ_{SFP} versus $X_{CoM_{SFP}}$, for vaults including 1 or 2 somersaults. As stated before, the database includes only one vault where 0 somersaults are performed, thus we will not include this in the automatic classification system. If we look at the perceived rotation between ϕ_{SFP} at $X_{CoM_{SFP}} = -1$, and ϕ_{SFP} at $X_{CoM_{SFP}} = 1$, we clearly see a distinction between the two classes. For one somersault the perceived rotation equals on average -500° . For two somersaults the perceived rotation equals on average -900° .

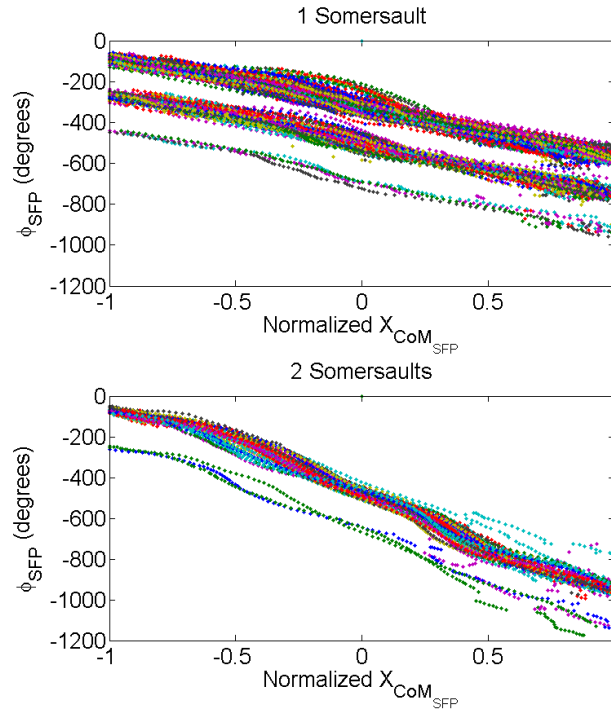


Figure 5.5 Normalized $X_{CoM_{SFP}}$ vs ϕ_{SFP} for the two Number of Somersaults classes.

Type of Somersault:

For the Type of Somersault section we only consider data occurring in the second flight phase. To align all the samples in space we normalized $X_{CoM_{SFP}}$. After investigating the particle measurements we locate regions of interest in the Hu Moment 1 ($Hu_{1_{SFP}}$), Rotated Bounding Rectangle Length 1 ($RBR1_{SFP}$) and in the Rotated Bounding Rectangle Length 2 ($RBR2_{SFP}$) particle measurements. Let us first consider $Hu_{1_{SFP}}$.

Figure 5.6 shows $Hu_{1_{SFP}}$ versus $X_{CoM_{SFP}}$, for the Tucked, Piked and Layout Type of Somersaults. Figure 5.6 shows that tucked and piked somersaults perceive a steep decline after the point of last hand contact ($X_{CoM_{SFP}} = -1$), followed by an approximately constant Hu Moment 1 throughout the rest of

the second flight phase. The layout type of somersaults shows a minor decline. Furthermore, the Hu Moment 1 is not constant throughout the rest of the vault.

Next we look at $RBR1_{SFP}$. Figure 5.7 shows $RBR1_{SFP}$ versus $X_{CoM_{SFP}}$, for the Tucked, Piked and Layout Type of Somersaults. If we look at Figure 5.7 we see the same trends as in Figure 5.6, for tucked and piked somersaults. Furthermore, notice that on average $RBR1_{SFP}$ for the layout somersaults is higher than that of tucked and piked somersaults.

Finally we look at $RBR2_{SFP}$. Figure 5.8 shows $RBR2_{SFP}$ versus $X_{CoM_{SFP}}$, for the Tucked, Piked and Layout Type of Somersaults. Looking at Figure 5.8 reveals that $RBR2_{SFP}$ for piked somersaults is on average higher than that of tucked somersaults.

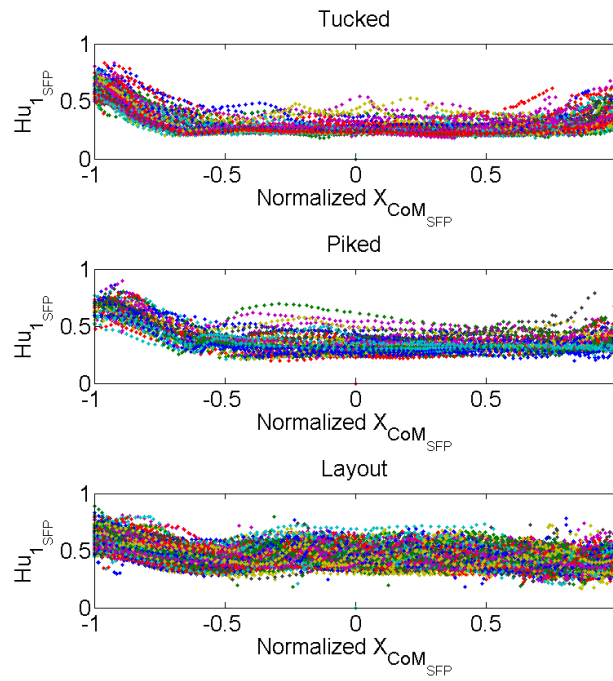


Figure 5.6 Normalized $X_{CoM_{SFP}}$ vs $Hu_{1_{SFP}}$ for the three Type of Somersaults classes.

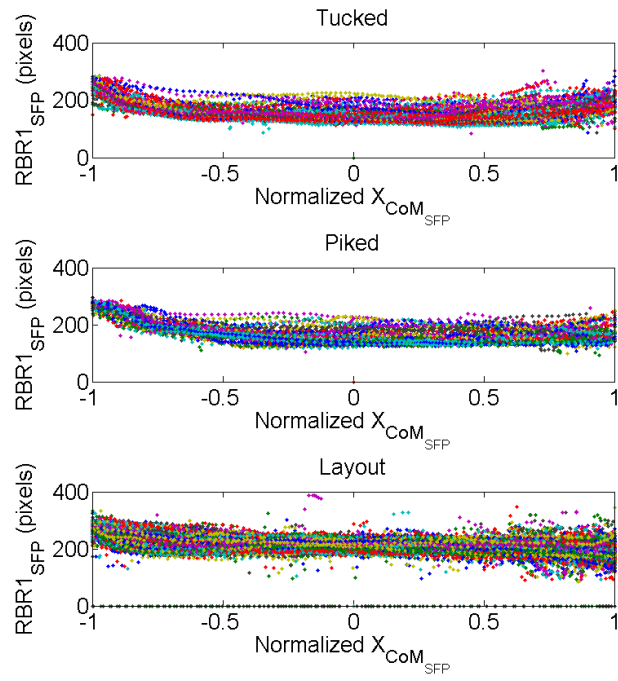


Figure 5.7 Normalized $X_{CoM_{SFP}}$ vs $RBR1_{SFP}$ for the three Type of Somersaults classes.

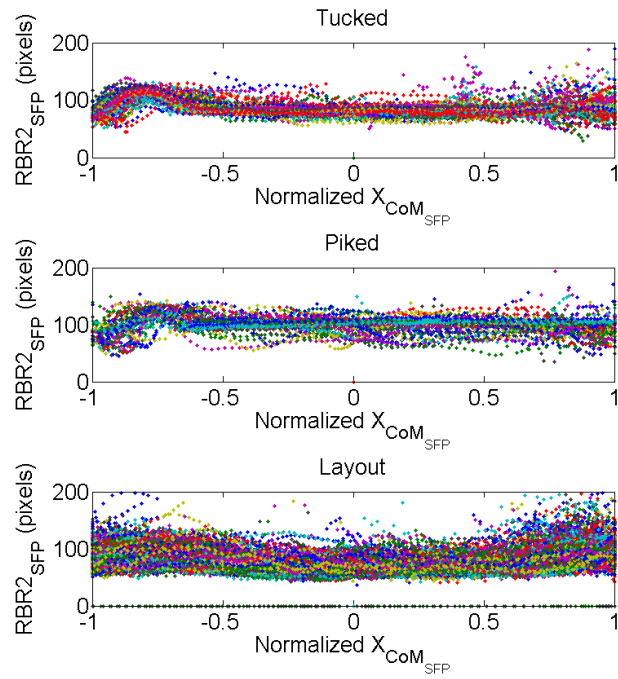


Figure 5.8 Normalized $X_{CoM_{SFP}}$ vs $RBR2_{SFP}$ for the three Type of Somersaults classes.

Number of Twists

For the Number of Twists vault-section we only consider data occurring in the second flight phase. After investigating the particle measurements we locate regions of interest in the Area (A_{SFP}) and in the Hu_{1SFP} particle measurements.

Figure 5.9 shows A_{SFP} versus $X_{CoM_{SFP}}$, for vaults including 0, 0.5, 1, 1.5, 2 or 2.5 twists. Each class shows a specific trend. A higher degree of twists induces more oscillations in A_{SFP} . However, there is a large inner-class variance. To magnify the specific class trends, A_{SFP} is normalized to $[-1,1]$. Figure 5.10 shows the normalized A_{SFP} versus the normalized $X_{CoM_{SFP}}$.

Figure 5.11 shows Hu_{1SFP} versus $X_{CoM_{SFP}}$, for vaults including 0, 0.5, 1, 1.5, 2 or 2.5 twists. We notice that, as for A_{SFP} , a higher degree of twists induces more oscillations in Hu_{1SFP} . However, there is a large inner-class variance. To magnify the specific class trends, Hu_{1SFP} is also normalized. Figure 5.12 shows the normalized Hu_{1SFP} versus the normalized $X_{CoM_{SFP}}$ for all the Number of Twists classes.

Figure 5.10 and Figure 5.12 show that the specific class trends are more refined. However, a large inner-class variance is still present. This is due to the fact that twisting is very actor specific, meaning that gymnasts have different twisting styles, which are initiated at different moments within the second flight phase. The overall trends of the normalized A_{SFP} and Hu_{1SFP} , maintain a positive linear relation between the number of oscillations and the number of twists.

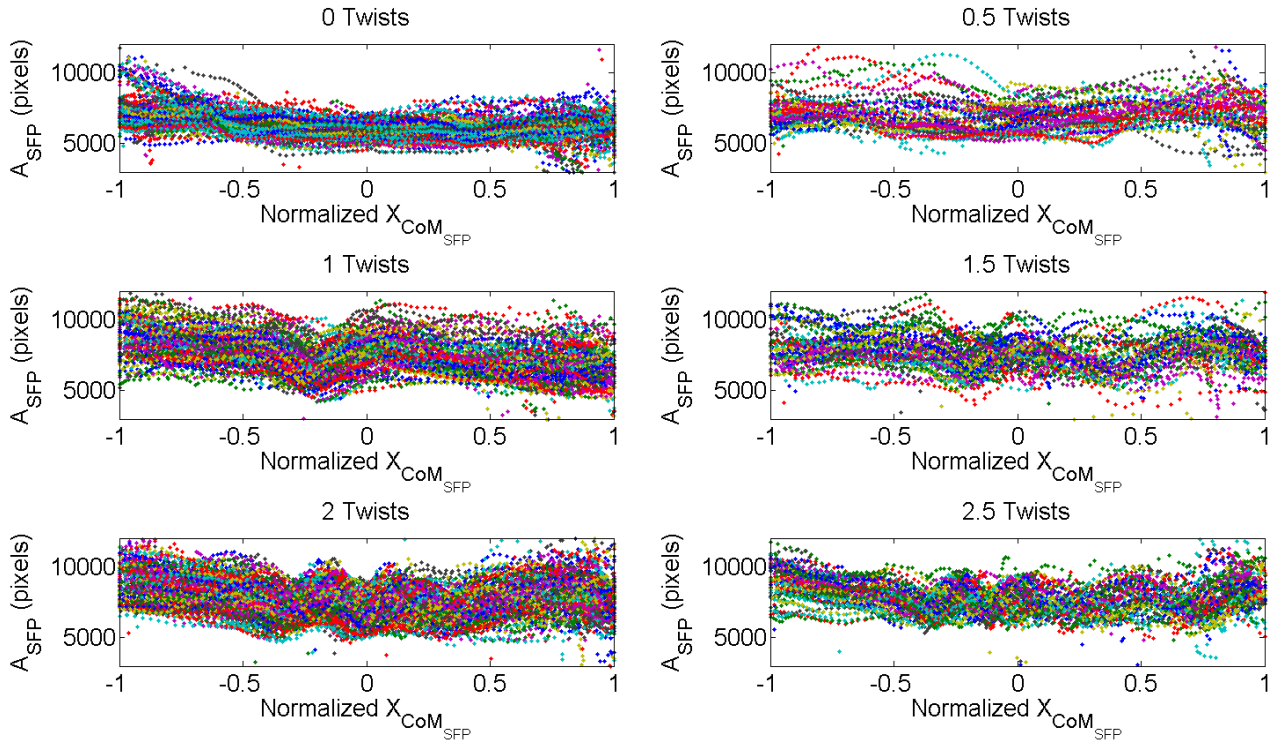


Figure 5.9 Normalized $X_{CoM_{SFP}}$ vs A_{SFP} for the six Type of Somersaults classes.

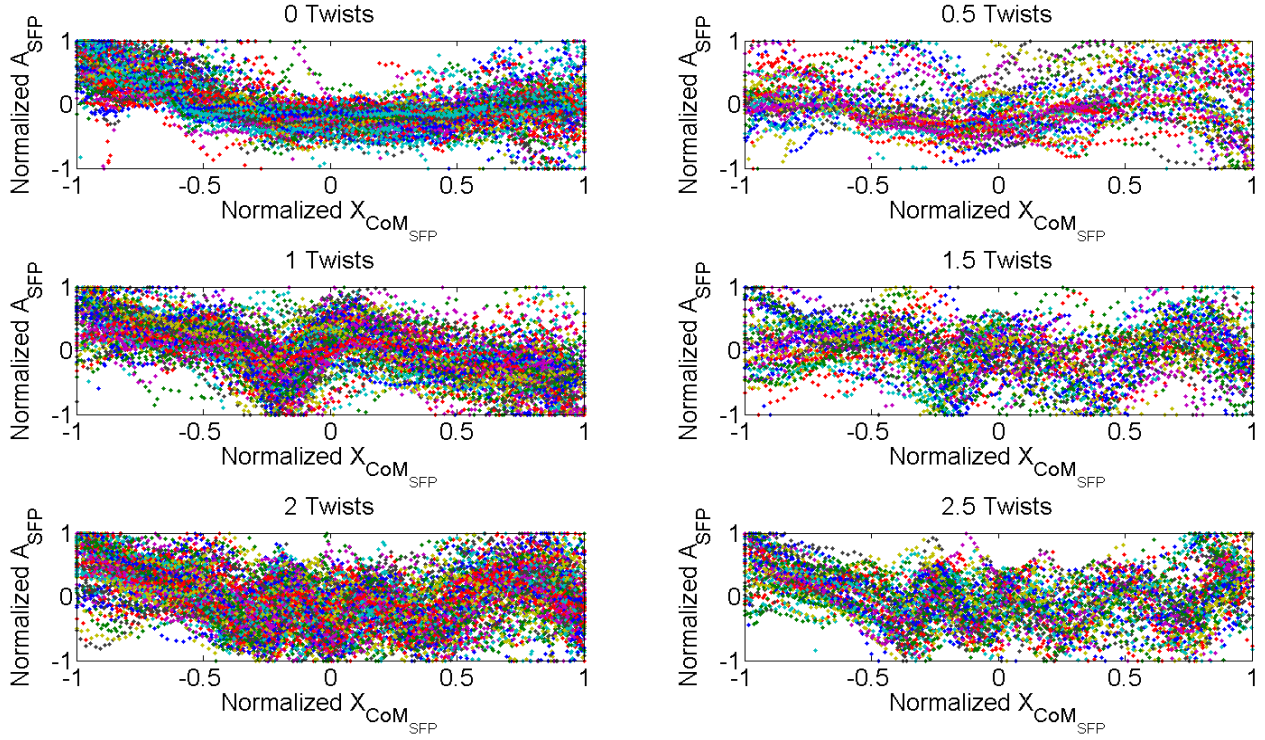


Figure 5.10 Normalized $X_{CoM_{SFP}}$ vs normalized A_{SFP} for the six Type of Somersaults classes.

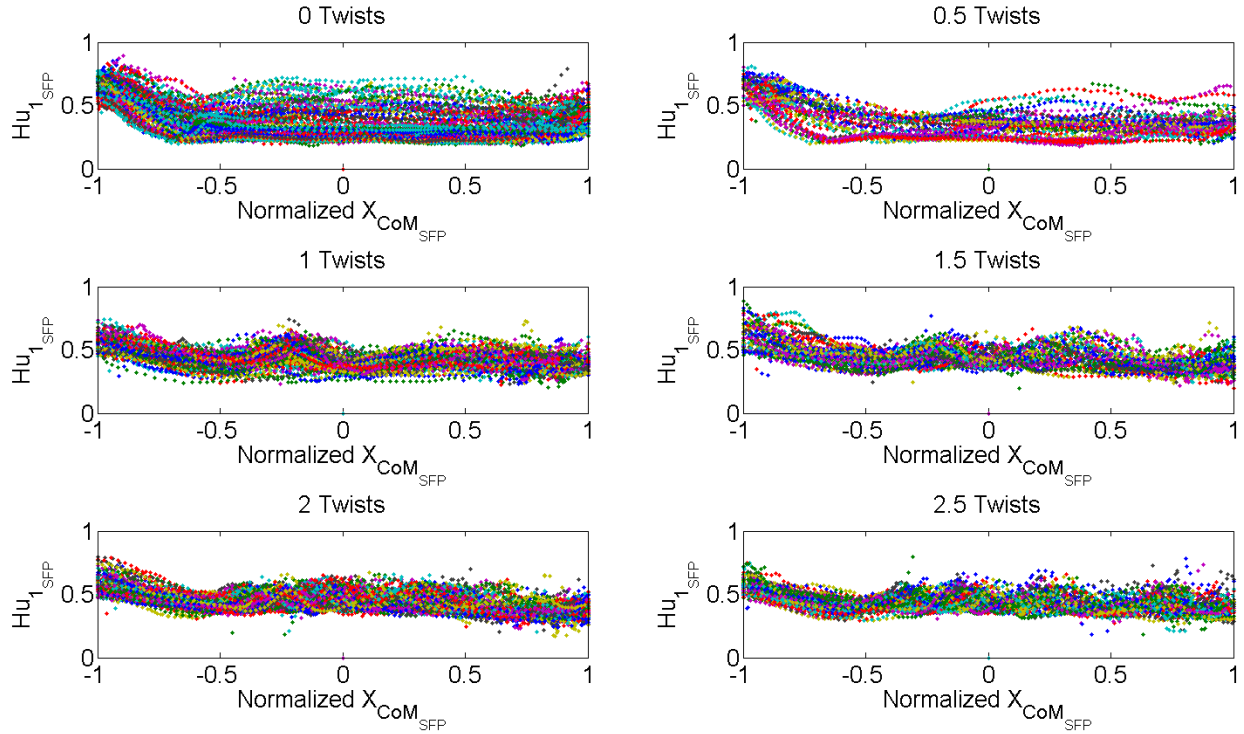


Figure 5.11 Normalized $X_{CoM_{SFP}}$ vs $Hu_{1_{SFP}}$ for the six Type of Somersaults classes.

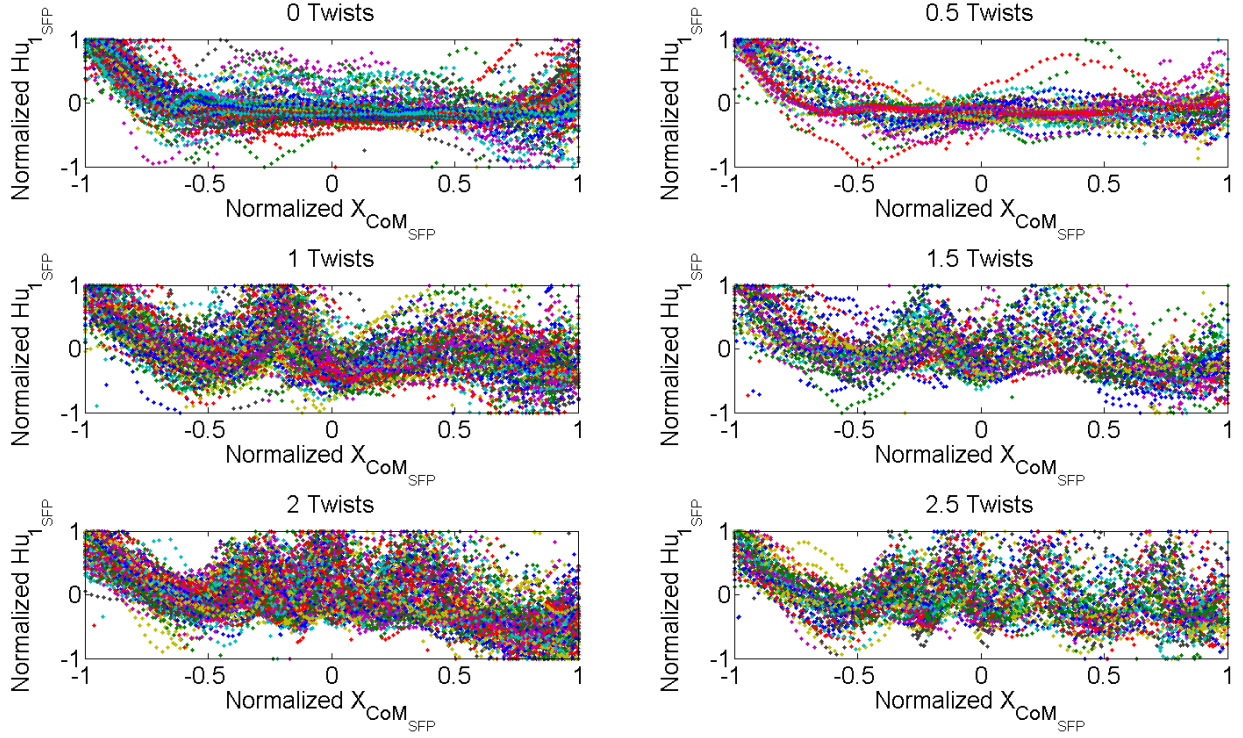


Figure 5.12 Normalized $X_{CoM_{SFP}}$ vs normalized $Hu_{1_{SFP}}$ for the six Type of Somersaults classes.

5.1.2 Physical Explanation

Type of Vault:

We can explain the differences in \emptyset_{FFP} by looking at what defines the Yurchenko and Yurchenko 1/2 type of vaults from the other vault types and by looking at the recordings. First of all, Yurchenko and Yurchenko 1/2 type of vaults include a round-off in the preparation phase. Looking at the recordings reveals that when a round-off is performed, the gymnast enters the range of the camera in an upside down position, thus with his hands on the ground. The Handspring and Tsukahara on the other hand include a hurdle jump in the preparation. The recordings reveal that for Handspring and Tsukahara type of vaults, gymnasts enter within the range of the camera in a straight up position. For all the vault types, the spring board is hit feet first. Furthermore, at the point of last hand contact, a gymnast is in an upside down position. During a Yurchenko or a Yurchenko 1/2 type of vault, a gymnast thus performs a full rotation before the point of last hand contact, which corresponds with the -400° in \emptyset_{FFP} . Furthermore, the gymnast rotates throughout the entire FFP. For the Handspring and Tsukahara type of vaults the gymnast performs a half rotation in FFP, corresponding to the -200° in \emptyset_{FFP} . Furthermore, the rotation is initiated at the take-off from the spring board.

For the physical explanation of the trends of the normalized A_{FFP} , we first notice that the deformation of the springboard, as well as the deformation of the vaulting table, is also picked up by the TTCP. This corresponds with the increase of A_{FFP} at $X_{CoM_{FFP}} = 0$ and $X_{CoM_{FFP}} = 0.8$, see Figure 5.4. To explain the differences in trends, we again look at what movements separate the different type of vault classes.

Yurchenko 1/2 type of vaults include a 1/2 twist in the first flight phase, whereas the Yurchenko type of vaults includes no twists. Furthermore, Tsukahara type of vaults include a 1/4 twist in the first flight phase, whereas the Handspring type of vaults include no twists. As stated before, the camera records the motions in a sagittal plane. When the gymnast performs no twists, only the sagittal plane of the body of the gymnasts is observed. When a 1/4 twist is performed the observation of the body of the gymnasts has moved from the sagittal plane (side view) to the coronal plane (front view). For an upright posture the area of the body in the coronal plane is larger than the area of the body in the sagittal plane. This results in the non-dipping effect in the Tsukahara and Yurchenko 1/2 type of vaults.

Number of Somersaults:

The perceived rotation of approximately -500° for one somersault vaults, corresponds with the rotation made between the point of last hand contact and the landing. This includes a full -360° rotation from the somersault, plus a rotation from an upside down position to a landing on the feet. Vaults including two somersaults perceive a rotation of approximately -900° . This is a full -360° larger than vault including one somersault, corresponding to the extra somersault made. Furthermore, the two somersaults samples show a slightly steeper decline in \emptyset_{SFP} , indicating that the rotational speed is higher. We notice a wide spread in Figure 5.5. All the class samples show a similar perceived rotation. However, some samples are initiated a 200° lower. This corresponds to the perceived rotation in the Type of Vault vault-section. Normalizing eliminates this spread. However, this also eliminates the absolute values of the perceived rotations in the second flight phase.

Type of Somersaults:

The decline in $Hu_{1_{SFP}}$, for tucked and piked somersaults, is explained by the physical interpretation of the Hu Moment 1, namely that the Hu Moment 1 represents the normalized moment of inertia about the local z-axis, which is perpendicular to the image. Furthermore, the Hu Moment 1 is rotational, space and size invariant. The Hu Moment 1 however does vary by the shape of the object, thus by different types of somersault postures. The decline in tucked and piked somersaults is due to the shape transition of a stretched body posture, at the point of last hand contact, to the tucked or piked body posture. The decline in $RBR1_{SFP}$ is due to same shape transition. Furthermore, the length of the body of the gymnast is for a layout somersault significantly greater than that of tucked and piked somersaults, thus on average, $RBR1_{SFP}$ is greater for layout somersaults than for tucked and piked somersaults.

The difference in $RBR2_{SFP}$ between piked and tucked somersaults is due to the width difference between the piked body posture and that of the tucked body posture in the x-y plane. The width difference is due to the stretched legs in the piked body posture.

Number of Twists:

The linear relation between the oscillations and the number of twists can be explained by the same physics as the non-dipping effect in A_{FFP} of the Tsukahara and Yurchenko 1/2 type of vaults. A 1/2 twist includes the rotation of the body from the sagittal plane to the coronal plane and back, which corresponds to a single oscillation.

5.2 Feature Selection

In the feature selection stage, the vault-section feature spaces have been reduced to a minimum by transforming the feature space X to feature set F , $X = (x_1, x_2, \dots, x_p) \in \mathbb{R}^{M \times P} \mapsto F \in \mathbb{R}^{1 \times f}$, where f is the length of the reduced feature set F . This is done to reduce the dimensionality of the problem, thus simplifying the problem. The reduction is performed by transformation mappings.

5.2.1 Transformation Mappings

For this thesis, three different transformation mappings are applied, namely: *Delta Features*, *Principal Component Analysis* and *Dynamic Time Warping*. Each mapping has its own strengths and weaknesses for reducing the feature space while obtaining a high discriminative power. Before the mappings are applied, the temporal variations between samples are resolved. Applying a Splines-fit to the regions of interest and sampling the spline-fit ($N=100$) ensures equal sizes for all the vault-section matrices, $X \in \mathbb{R}^{M \times P} \mapsto X \in \mathbb{R}^{M \times N}$. Furthermore, the particle measurements are prone to noise. The Principal Component Analysis mapping, and possibly the Dynamic Time Warping mapping, are biased by the noise, decreasing the discriminative power of the resulting feature sets. To smoothen the particle measurements, a low pass third-order Butterworth filter (cut-off frequency of 0.2) is applied to the regions of interest, before presenting these to the relevant transformation mappings.

Delta Features:

The Delta Features mapping is the most simple, where we use reasoning and simple algebraic operators to generate new features from the vault-section feature matrices. The delta feature set is optimized by a leave-one-out principle, using the classification error estimate as performance measure. The advantage of this mapping is that the Delta Features represent the physical explanations of the regions of interest, while reducing the feature space to a minimum. However, this method is not robust against interclass and local time variations.

Principal Component Analysis (PCA):

PCA converts the possibly correlated feature space into a feature set of uncorrelated features, called *principal components*. PCA assumes that the highest discriminative principal components are found in the direction of the largest variance of the feature space. Furthermore, the principal components are constrained to be orthogonal to each other. In this thesis, the principle components cover 99% of the variance within the regions of interest. This mapping is susceptible to inner-class variations. To improve the PCA mapping, the regions of interest are firstly smoothened by the Butterworth filter.

Dynamic Time Warping:

The third mapping uses a dynamic programming algorithm known as *Dynamic Time Warping (DTW)* to generate Motion Templates (**MT**). This mapping does not reduce the feature space but it generates a general motion template, representing the motion characteristics. The general motion template is used as reference feature matrix for the Dynamic Time Warping classifier, discussed in section 5.3. It is thought that the DTW algorithm is more robust against inner-class and local variations. The drawback of this mapping is that it is computational expensive. For a better understanding of the power of the DTW

mapping, a general discussion of the DTW algorithm and Motion Templates is given below. For a detailed discussion of the DTW algorithm and Motion Templates, we refer the reader to [17] [20].

DTW algorithm: DTW locally stretches and compresses feature matrix X to match a reference feature matrix X_{ref} . A similarity measure is used to compare X to X_{ref} , resulting in a cost matrix. For this thesis the Euclidian distance, $\|x - y\|$, is used as similarity measure. By dynamic programming, an optimal warping path can be subtracted from the cost matrix. By summing up the cost values that lie within the warping path, the warping cost is obtained. The warping path is optimized to obtain the minimal warping cost. The optimal warping path defines the local stretching and compressing of feature matrix X , to best match X_{ref} . The warping cost defines the similarity of X to X_{ref} , where a low warping cost defines a high level of similarity.

Motion Templates: A motion template is created by choosing one class sample to act as reference, use DTW to transform the remaining class samples such that they best match the reference sample and average over all the transformed samples. By this the motion template summarizes the motion characteristics of all the class samples. However, the motion template is biased by the reference sample. To ensure that the general motion template represents the motion characteristics best and is not biased by the reference class sample, each class sample is chosen as reference signal, resulting in an equal amount of motion templates as class samples. The motion template with the minimal cost represents the motion characteristics best. While the motion template summarizes the motion information of all the class samples it is still biased by the reference sample. The biasing is resolved by iteratively repeating the process, where the resulting motion templates from the previous iteration step serve as input for the current iteration step. This iteration continues until the minimal warping cost becomes smaller than 0.5.

5.2.2 Reduced Feature Sets

The application of the transformation mappings results in a reduced feature set. Due to the computational expense of the Dynamic Time Warping mapping, we only applied DTW for vault-sections containing a high inner-class variation in the regions of interest. The delta features below are the optimized delta features.

Type of Vault (TV):

The regions of interest for the Type of Vault vault-section are \emptyset_{FFP} and A_{FFP} . Furthermore, the normalized \emptyset_{FFP} and A_{FFP} show specific trends.

Delta Feature: The delta features D_{TV} are extracted from \emptyset_{FFP} and A_{FFP} and are shown in Table 5.1. D_{1TV} represents the perceived rotation and is defined by the difference between \emptyset_{FFP} at 95% and 5%. D_{2TV} represents the average of A_{FFP} between 60% and 80%. D_{3TV} defines the relative difference between the area of the body before hitting the vaulting board and after take-off from the vaulting board.

Table 5.1 Delta Feature Set for the Type of Vault vault-section.

Feature	Definition
D_{1TV}	$\phi_{95\%FFP} - \phi_{5\%FFP}$
D_{2TV}	$A_{60-80\%FFP}$
D_{3TV}	$A_{60-80\%FFP} - A_{5-20\%FFP}$

PCA: The PCA mapping is based on the normalized regions of interest. Before applying the PCA mapping, the regions of interest are filtered by the Butterworth filter. The PCA mapping transforms the feature space into 14 principle components, $X_{TV} \in \mathbb{R}^{2 \times 100} \mapsto PCA_{TV} \in \mathbb{R}^{1 \times 14}$.

Dynamic Time Warping: The DTW mapping was performed on two different feature sets. The first feature set includes the normalized ϕ_{FFP} and A_{FFP} . This results in the general template $Temp1_{TV}$. The second feature set includes the Butterworth filtered normalized ϕ_{FFP} and A_{FFP} . This results in the general template $Temp2_{TV}$. On average, 9 iterations are needed to obtain a warping cost lower than 0.5. The DTW mapping is computational expensive and slow, with an average computational time of over 2 hours.

Number of Somersaults (NS):

The region of interest for the Number of Somersaults vault-section is ϕ_{SFP} .

Delta Feature: The delta features D_{NS} are shown in Table 5.2. D_{1NS} represents the perceived rotation during the second flight phase. It is defined by the difference between ϕ_{SFP} at 1% and 99 %. D_{2NS} , D_{3NS} and D_{4NS} cover the difference in rotational speed between vaults including one and two somersaults.

Table 5.2 Delta Feature Set for the Number of Somersaults section.

Feature	Definition
D_{1NS}	$\phi_{99\%SFP} - \phi_{1\%SFP}$
D_{2NS}	$\phi_{5\%SFP}$
D_{3NS}	$\phi_{50\%SFP}$
D_{4NS}	$\phi_{95\%SFP}$

PCA: The PCA mapping transforms the butterworth filtered ϕ_{SFP} into 3 principle components, $X_{NS} \in \mathbb{R}^{1 \times 100} \mapsto PCA_{NS} \in \mathbb{R}^{1 \times 3}$.

Dynamic Time Warping: Because the inner-class variance in the regions of interest is small, no DTW mapping is generated.

Type of Somersault (TS):

The regions of interest for the Type of Somersault vault-section are $Hu_{1_{SFP}}$, $RBR1_{SFP}$ and $RBR2_{SFP}$.

Delta Feature: The delta features D_{TS} are shown in Table 5.3. $D_{1_{TS}}$ and $D_{2_{TS}}$ represent the decline in $Hu_{1_{SFP}}$. $D_{3_{TS}}$ and $D_{4_{TS}}$ represent the decline in $RBR1_{SFP}$. $D_{5_{TS}}$ represents the average width of the body posture during 30% to 70% of the second flight phase.

Table 5.3 Delta Feature Set for the Type of Somersaults section.

Feature	Definition
$D_{1_{TS}}$	$\overline{Hu1_{1-5\%SFP}}$
$D_{2_{TS}}$	$\overline{Hu1_{1-5\%SFP}} - \overline{Hu1_{30-70\%SFP}}$
$D_{3_{TS}}$	$\overline{RBR1_{1-5\%SFP}}$
$D_{4_{TS}}$	$\overline{RBR1_{1-5\%SFP}} - \overline{RBR1_{30-70\%SFP}}$
$D_{5_{TS}}$	$\overline{RBR2_{30-70\%SFP}}$

PCA: The PCA mapping transforms the Butterworth filtered $Hu_{1_{SFP}}$, $RBR1_{SFP}$ and $RBR2_{SFP}$ into 20 principle components, $X_{TS} \in \mathbb{R}^{3 \times 100} \mapsto PCA_{TS} \in \mathbb{R}^{1 \times 20}$.

Dynamic Time Warping: Because the inner-class variance in the regions of interest is small, no DTW mapping is generated.

Number of Twists (NT):

The regions of interest for the Number of Twists vault-section are the normalized A_{SFP} and $Hu_{1_{SFP}}$.

Delta Feature: No meaningful delta features can be generated due to the large inner-class variance in the regions of interest.

PCA: The normalized A_{SFP} and $Hu_{1_{SFP}}$ show a large inner class variance. To explore the discriminative power of the discriminative power of A_{SFP} and $Hu_{1_{SFP}}$, the PCA mapping is applied to each particle measurement individually, as well as to the combined feature set. The three resulting feature sets are composed of 15, 15 and 27 principal components, see Table 5.4.

Table 5.4 Principal Component Analysis Feature sets for the Number of Twists section.

Regions of interest	PCA feature set
$A_{SFP} \in \mathbb{R}^{1 \times 100}$	$PCA1_{NT} \in \mathbb{R}^{1 \times 15}$
$Hu_{1_{SFP}} \in \mathbb{R}^{1 \times 100}$	$PCA2_{NT} \in \mathbb{R}^{1 \times 15}$
$[A_{SFP}, Hu_{1_{SFP}}] \in \mathbb{R}^{2 \times 100}$	$PCA3_{NT} \in \mathbb{R}^{1 \times 27}$

Dynamic Time Warping: The DTW mapping was performed on two different feature sets. The first feature set includes the normalized A_{SFP} and normalized $Hu_{1_{SFP}}$ was used. This resulted in the general template $Temp1_{NT}$. The second feature set includes the Butterworth filtered normalized A_{SFP} and normalized $Hu_{1_{SFP}}$. This results in the general template $Temp2_{NT}$.

5.3 Classifiers

In this thesis, the Matlab PR-toolbox (version 4.2.1), developed by The Pattern Recognition Research Group of the TU Delft [19], is used for the design of 12 standard classifiers. The default settings of the PR-toolbox are kept during the design of the classifiers. Furthermore, a 13th classifier, which is not included in the PR-toolbox, is designed, allowing for a classification based on the Dynamic Time Warping algorithm. The classifiers range from simple linear classifiers, to complex, highly nonlinear classifiers. The data sets, presented in this thesis, are presented to the classifiers with equal class priors, except for the DTW classifier.

The classifier is the algorithm that maps the reduced feature sets to the vault-section class labels. The mapping consists of generating a decision boundary, which separates the feature space into class regions. Each class region is assigned a class label. In addition to the class labels proposed in section 4.1, a “reject” class is added to each vault-section. The decision boundary is extended with a rejection boundary, by applying the Matlab function *rejectc* (included in the PR-toolbox). *rejectc* supports ambiguity rejection and outlier rejection. The differences between ambiguity rejection and outlier rejection are best shown in Figure 5.13 and Figure 5.14. Samples that lie between the rejection boundary and the decision boundary are labeled as rejected. The complexity of the rejection curve depends on the complexity of the classifier. Outlier rejection is preferred over ambiguity rejection, where only samples that lie near the decision boundary are rejected. However, the used version of the PR-toolbox does not yet support outlier rejection for every classifier. Furthermore, outlier rejection risks overfitting the rejection boundary for higher order feature spaces. Therefore, in chapter 6, both rejection types will be evaluated.

In this study 13 classifiers have been evaluated. Below, an overview of these classifiers with their default settings and the accompanying PR-toolbox matlab functions (between brackets) are given. For a detailed explanation of the classifiers the reader is referred to the PR-toolbox website [19], or the book “Pattern Recognition”, by Theodoridis et al. [9].

- 1) Nearest Mean Classifier (nmc). A linear classifier that is insensitive to class priors but feature scaling sensitive. Outlier rejection is not supported.
- 2) Linear Bayes Normal Classifier (ldc). A linear classifier which assumes normal densities of the classes. No regularization parameters are added to the classifier. Outlier rejection is supported.
- 3) Fisher's Least Square Linear Classifier (fisherc). A linear classifier that uses least squares for determining the separation boundary. The classifier is non-density based, thus does not make use of the prior class probabilities. Outlier rejection is not supported.
- 4) Logistic Linear Classifier (loglc). A linear regression classifier which uses logistic (sigmoid) functions to maximize the likelihood criterion. Outlier rejection is not supported.

- 5) Support Vector Classifier (svc). Quadratic programming is used to optimize the classifier. The non-linearity of the classifier is determined by the kernel. A linear kernel is used as the default kernel.
- 6) Optimized Parzen Classifier (parzenc). A nonlinear classifier which is optimized in the smoothing parameter. Outlier rejection is supported.
- 7) K-Nearest Neighbor Classifier (knnnc). A nonlinear classifier, defining the classification boundary by the distance between a training sample and its k-nearest neighbors. K is optimized with respect to the leave-one-out error on TRN. Outlier rejection is not supported.
- 8) Quadratic Bayes Normal Classifier (qdc). A quadratic classifier which assumes normal densities of the classes. No regularization parameters are added to the classifier. Outlier rejection is supported.
- 9) Parzen Density Based Classifier (parzendc). A parzen classifier for which the smoothing parameters are based on the estimate of the class densities from TRN. Outlier rejection is supported.
- 10) Decision Tree Classifier (treec). Uses a binary splitting criterion. Default is purity, no pruning.
- 11) Linear perception classifier (perlc). A linear perception with learning rate 0.1. The weights of the perception are set by random initialization. Training is performed until convergence of the classifier, or when the maximum number of iterations is met (default 100). The classifier is updated by batch processing.
- 12) Back-Propagation Trained Feed-Forward Neural Network Classifier (bpxnc). A neural network that is trained using the back-propagation algorithm. Number of neurons per hidden layer is set to 5. Weight initialization is performed by Matlab's neural network toolbox. Tuning is performed on TRN. Training is stopped when the number of iterations exceeds twice that of the best classification result.
- 13) Dynamic Time Warping Classifier. Dynamic time warping is used, where the general motion templates serve as references. The classification is made on the minimal warping cost. The difference between the lowest and the second lowest warping cost is depicted by DIFF. A sample is rejected if DIFF is lower than 5% of the lowest warping cost.

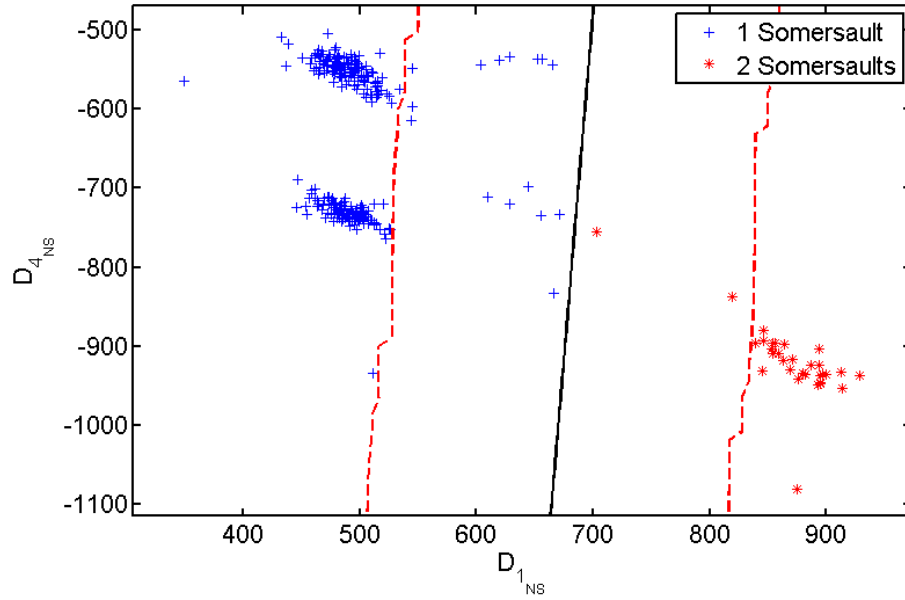


Figure 5.13 Scatter plot of Number of Somersault features $D_{1_{NS}}$ (x-axis) and $D_{2_{NS}}$. The blue plusses indicate the TRN samples belonging to the 1 Somersault label. The red asterisks indicate the TRN samples belonging to the 2 Somersaults label. The black line indicates the decision boundary made by the Linear Bayes Normal Classifier. The red striped lines indicate the rejection boundaries made by ambiguity rejection. 5% of the TRN samples is rejected.

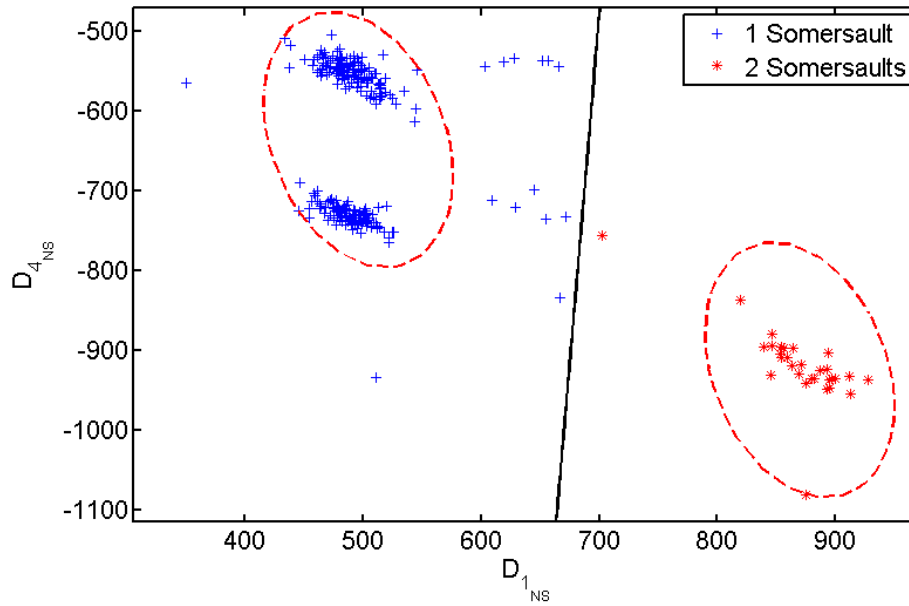


Figure 5.14 Scatter plot of Number of Somersault features $D_{1_{NS}}$ (x-axis) and $D_{2_{NS}}$. The blue plusses indicate the TRN samples belonging to the 1 Somersault label. The red asterisks indicate the TRN samples belonging to the 2 Somersaults label. The black line indicates the decision boundary made by the Linear Bayes Normal Classifier. The red striped lines indicate the rejection boundaries made by outlier rejection. 5% of the TRN samples is rejected.

6 Vault-section Evaluation

The remaining chapters of this thesis cover the final design step of the classification system; the evaluation of the system. This includes the evaluation of the vault-section classifications and the validation of the classification system for complete vault jumps.

In chapter 5, several reduced features sets (Delta feature set, PCA feature set, DTW feature set) were proposed for each vault-section. Furthermore, different rejection types and a variety of classifiers have been given. The combination of these defines the performance of the classification. For classifying the entire motion sequence of a vault jump, the overall performance is bound by the classification performances of the vault-sections, meaning that the performance is at most as good as the performance of the vault-section with the lowest classification rate. Therefore, we will first evaluate the classification performance of each vault-section individually, before evaluating the classification of a complete vault.

This chapter treats the experiments applied on the WC 2010 database to evaluate the individual vault-sections. The evaluation experiments are introduced in section 6.1. A general evaluation process is designed to choose the best reduced feature set - classifier - rejection combination per vault-section. The best combination involves the reduced feature set that best represents the characteristics of the vault-section-classes, and the classifier - rejection combination that is best able to separate the vault-section-classes while keeping the number of rejections low. In section 6.2, the general evaluation process is applied to the vault-sections “Type of Vault”(TV), “Number of Somersaults”(NS), “Type of Somersault”(TS) and “Number of Twists”(NT) resulting in the best combination per vault-section. Section 6.3, concludes the vault-section evaluation. The four chosen vault-section combinations are used for the validation of the system in chapter 7.

6.1 Evaluation Experiments

The classification method must be trained and evaluated on independent feature sets. To provide this, the database is divided into an even split by randomly assigning 50% of the samples to the training database (TRN) and 50% of the samples to the evaluation database (TST). Table 6.1 shows the number of training and testing samples per vault-section-class. The 50-50 split allows us to investigate what influence the individual components of the reduced feature set - classifier - rejection combination have on the classification performance of the combination. This is done by computing the classification error estimate, rejection curve and confusion matrix for each combination.

The classification error estimate is the average of the misclassification rates per class. This experiment gives an initial estimate of the classification error without rejection. The rejection curve relates the classification error on TST to the percentage of rejected samples of TRN, thus gives insight in the rejection properties of the reduced feature set - classifier combination. The classification error does not include rejected samples of TST, thus is based on the count of misclassified samples and the total number of classified samples. Furthermore, the rejection curve is based on ambiguity rejection. The goal of an automatic vault classification system is to reduce the manual labor in classifying vault jumps recordings, thus a high rejection rate is inadequate.

To give a more detailed insight in the classification performance and the rejection rate on TST, confusion matrices are computed. Confusion matrices relate the true class labels (rows) to the estimated class labels (columns). The diagonal entries of the confusion matrix, where the estimated class labels correspond to the true class labels, indicate the correct classified samples. The off-diagonal entries indicate the misclassified samples. The confusion matrices are applied to the reduced feature set - classifier combinations and to the reduced feature set - classifier - rejection combination.

The experiments on the 50-50 split database result in a selection of best performing combinations per vault-section. However, using only 50% of the data for training, results in an underestimation of the classification performance. Naturally, the best classification performance is obtained by using all data for training. However, using the same data for testing results in an overestimation of classification performance. To give a trustworthy estimation of the overall classification performance, bootstrapping experiments are performed. In bootstrapping, 10 randomly drawn samples from the WC 2010 database are used as test samples and the remaining samples are used for training. This ensures that the classifiers are trained in the optimal way. However, only using 10 samples for testing results in an unreliable error estimate. To give a reliable error estimate, the process is repeated 100 times, where for each repetition a new set of test samples is drawn and the classifiers are retrained. Drawback of bootstrapping is that it becomes extremely slow when applied to the computational expensive DTW-mapping. Furthermore, bootstrapping only gives information about the overall classification performance, thus provides no insight in the discriminative power of the individual components of the reduced feature set - classifier - rejection combinations. We will therefore use bootstrapping as validation method for the best performing combinations of the 50-50 split experiments. Remember that the 50-50 split experiments do give insight in the discriminative power of the individual components of the reduced feature set - classifier - rejection combinations.

Table 6.1 Table of training and testing samples per vault-section class.

Vault-sections	Vault-section-classes	Training samples, total=306	Test samples, total = 303
Type of Vault (TV)	Handspring Tsukahara Yurchenko Yurchenko 1/2	83 100 112 11	67 115 109 12
Number of Somersaults (NS)	1 2	273 32	278 25
Type of Somersault (TS)	Tucked Picked Layout	46 28 232	40 34 229
Number of Twists (NT)	0 0.5 1 1.5 2 2.5	66 25 68 32 79 36	65 25 67 31 79 36

6.2 Vault-Section Results

In this section we apply for each vault-section individually the previously mentioned evaluation experiments. This includes the computation of the error estimate, rejection curve and confusion matrix on the 50-50 split database, and the validation by bootstrapping. For ease of the reader, only the combinations that perform best in the 50-50 split and bootstrapping experiments will be treated. A summary of the results is given in Appendix A.

The bootstrap results include the correct classification rates (with and without rejection), misclassification rates (with and without rejection) and the rejection rate.

6.2.1 Type of Vault (TV) Classification

The TV-50-50 split experiments show (Appendix A.1) that the best results for the TV vault-section are provided by the Delta Feature mapping-Logistic Linear Classifier-Ambiguity rejection combination (D_{TV} -LOGLC-Amb5% = 16 misclassifications, 14 rejections), the PCA feature set-Linear Bayes Normal Classifier-Ambiguity rejection combination (PCA_{TV} -LDC-Amb5% = 8 misclassifications, 23 rejections), and the general template 1 feature set-Dynamic Time Warping classifier-Diff rejection combination ($Temp1_{TV}$ -DTW-Diff5% = 11 misclassifications, 11 rejections). All reduced feature set - classifier - rejection combinations show acceptable rejection and misclassification rate. The $Temp1_{TV}$ -DTW-Diff5% combination does not outperform the other combinations. Due to the computational expense involved in this combination, we did not evaluate this combination in the TV-bootstrap experiments.

Table 6.2 shows the results of the bootstrap experiments. It shows that the PCA_{TV} -LDC-Amb5% combination results in the lowest misclassifications rate while maintaining an acceptable rejection rate.

Table 6.2 TV-Bootstrap experiment results (1000 test samples).

Reduced feature set - classifier-combination	Correct classification rate (%)	Mis-classification rate (%)	Rejection type	Correct classification rate with rejection (%)	Mis-classification rate with rejection (%)	Rejection rate (%)
D_{TV} -LOGLC	91.7%	8.3%	Ambiguity (5%)	89.8%	6.7%	3.5%
PCA_{TV} -LDC	95.2%	4.8%	Ambiguity (5%)	91.2%	3.1%	5.7%

6.2.2 Number of Somersaults (NS) Classification

The NS-50-50 split experiments show (Appendix A.2) that all the reduced feature set - classifier - rejection combinations performed adequately in classifying the 1 and 2 somersaults classes, indicating a high discriminative power of the region of interest (\emptyset_{SFP}) and well separated classes in the feature space (see Figure 5.13 and Figure 5.14). As stated in section 4.1, we do not include the 0 somersaults class in the classification system. However, novice gymnasts generally perform vaults including 0 somersaults. These vaults are considered to be outliers, therefore, outlier rejection is preferred to ambiguity rejection for the NS vault-section. Furthermore, not all the classifiers support outlier rejection (Out). The best classification performances given by the combinations that include outlier rejection are

given by the Delta Feature set-Linear Bayes Normal Classifier-Outlier rejection combination (D_{NS} -LDC-Out5%, 0 misclassifications, 23 rejections), and the PCA mapping-Parzen density classifier-Outlier rejection (PCA_{NS} -PARZENDC-Out5%, 0 misclassifications, 11 rejections).

Table 6.3 shows the results of the NS-bootstrap experiments. The high number of training samples during bootstrapping in combination with the high discriminative power of \emptyset_{SFP} allows for lowering the rejection rate during training. The NS-bootstrap results show that the D_{NS} -LDC-Out1% combination performs best.

Table 6.3 NS-Bootstrap experiment results (1000 test samples).

Reduced feature set - classifier combination	Correct classification rate (%)	Mis-classification rate (%)	Rejection type	Correct classification rate with rejection (%)	Mis-classification rate with rejection (%)	Rejection rate (%)
D_{NS} -LDC	99.9%	0.1%	Outlier (1%)	98.1%	0.1%	1.8%
PCA_{NS} -PARZENDC	99.5%	0.5%	Outlier (1%)	97.0%	0.2%	2.8%

The high performance of all reduced feature set - classifier combinations indicates a high discriminative power in the regions of interest (\emptyset_{SFP}). This is substantiated by the fact that the PCA mapping is able to cover 99% of the variance in only three principal components. The D_{NS} -LDC-Out1% combination performs better than the PCA_{NS} -PARZENDC-Out1% combination. Furthermore, D_{NS} is preferred to PCA_{NS} because of the preserved physical interpretation of the feature set.

To check the rejection properties of the D_{NS} -LDC combination, a rejection experiment was performed. In this experiment the D_{NS} -LDC combination is trained on the complete database for both outlier and ambiguity rejection. The excluded sample containing 0 somersaults serves as test sample. When ambiguity rejection was applied, the test sample is labeled "2 somersaults". Using outlier rejection results in a successful rejection of the test sample.

6.2.3 Type of Somersault (TS) Classification

The TS-50-50 split experiments show (Appendix A.3) that for the classification of the TS vault-section the Delta feature set-Quadratic Bayes Normal Classifier-Outlier rejection combination (D_{TS} -QDC-Out5%, 10 misclassifications, 17 rejections), the Delta feature set-Parzen Density Classifier-Ambiguity rejection combination (D_{TS} -PARZENDC-Amb5%, 6 misclassifications, 22 rejections), the PCA feature set-k-nearest neighbor classifier-Ambiguity rejection combination (PCA_{TS} -KNNC-Amb5%, 14 samples misclassified, 2 samples rejected) and the PCA feature set-Parzen classifier-ambiguity combination (PCA_{TS} -PARZENC-Amb5%, 1 misclassifications, 44 rejections).

Table 6.4 shows the results of the bootstrap experiments. It shows that the misclassification rate, as well as the rejection rate, is best for D_{TS} -QDC-Out5%. While the misclassification rate of PCA_{TS} -KNNC-Amb5% is lower than that of D_{TS} -QDC-Out5%, the rejection rate of PCA_{TS} -KNNC-Amb5% is much

higher. Lowering the rejection rate during training did not lower the rejection rate of the PCA_{TS} -KNNC-Amb combination.

Table 6.4 TS-Bootstrap experiment results (1000 test samples).

Reduced feature set - classifier combination	Correct classification rate (%)	Mis-classification rate (%)	Rejection type	Correct classification rate with rejection (%)	Mis-classification rate with rejection (%)	Rejection rate (%)
D_{TS} -QDC	96.1%	3.9%	Outlier (5%)	91.8%	2.8%	5.4%
D_{TS} -PARZENDC	93.7%	6.3%	Ambiguity (5%)	87.0%	2.2%	10.8%
PCA_{TS} -PARZENC	92.1%	7.9%	Ambiguity (5%)	88.9%	4.6%	6.5%
PCA_{TS} -KNNC	96.8%	3.2%	Ambiguity (5%)	65.6%	1.2%	33.2%

The bootstrap experiments show that the generalization performance of the k-nearest neighbor classifier with outlier rejection is low. In general, more complex classifiers risk overfitting the rejection boundary if applied to higher order feature spaces. It is thought that the rejection boundary of KNNC does not only separate the different classes, it also separates clusters of equal classes. By this, a class region is not confined to one cluster but exists of numerous clusters. Samples that lie outside the clusters are rejected. This is substantiated by the results of the NT and TV 50-50 split experiments. Why KNNC performed adequately in the TS-50-50 split experiment is unclear.

6.2.4 Number of Twists (NT) Classification

As stated in section 5.2, due to the high inner class variations in the NT-regions of interest no meaningful Delta Features could be derived to determine the number of performed twists in the second flight phase. Furthermore, to thoroughly investigate the discriminative power of the regions of interest (A_{SFP} , $Hu_{1_{SFP}}$) the PCA transformation mapping is applied to the regions of interest separately and combined, resulting in three PCA feature sets. In addition to this, two DTW mappings were applied.

The NT-50-50 split experiments (Appendix A.4) show that the Parzen classifier performed optimal for all PCA mappings. Furthermore, lowering the rejection rate during training significantly lowers the rejection rate of test samples with a minor increase in the amount of misclassifications. Overall, the $PCA3_{NT}$ -PARZENC-Ambiguity combination performs best for the classification of the number of twists.

The NT-bootstrap experiments give the same result as the 50-50 split experiments, namely that the best performance is provided by the PCA3 feature set-Parzen classifier-Ambiguity rejection combination ($PCA3_{NT}$ -PARZENC-Amb1%, 13 misclassifications, 63 rejections).

6.3 Conclusion

By the 50-50 split experiments, we have gained insight into the discriminative power of the regions of interest, as well as the discriminative power of the reduced feature sets. Furthermore, the bootstrap experiments give a valid estimate of the overall classification performances of the individual vault-section classifications. The main results are as followed.

The Delta feature mapping is best for the NS and TS vault-sections, which show a low inner-class variance in their regions of interest. Furthermore the regions of interest of NS and NT are represented by signals with a low degree of fluctuations. This allows for defining low dimensional delta feature sets ($D_{NS} \in \mathbb{R}^{1 \times 4}$, $D_{TS} \in \mathbb{R}^{1 \times 5}$) that contain a high discriminative power. The Delta features are based on simple algebraic operations and are therefore less powerful for regions of interest containing a fluctuating signal or high inner-class variances.

Both the TV and NT vault-sections regions of interest include fluctuating signals, accompanied by a high inner-class variance. The PCA mapping used in this thesis, includes a Butterworth filter, which smoothens the regions of interest and reduces the inner-class variance. Instead of focusing on the inner-class variance, the PCA mapping now focuses on the fluctuations in the regions of interest, which define the different vault-section-classes. The vault-section evaluation experiments show that the PCA mapping performs best for the TV and NT regions of interest.

The PCA_{TV} -LDC-Amb5%, D_{NS} -LDC-Out1%, D_{TS} -QDC-Out5% and $PCA3_{NT}$ -PARZENC-Amb1% combinations turn out to be the best performing combinations of all tested combinations, and are thus applied in the complete vault classification evaluation. Table 6.5 shows the bootstrap experiment results of these four best performing vault-section combinations. All the combinations show a misclassification rate below the 5% (with rejection). The correct classification rate without rejection for the NT combination is the lowest (88.9%), thus the best performance of the complete vault classification system is at most capable of correctly classifying 88.9% of all samples.

Table 6.5 Summary of the bootstrap results of the four best performing vault-section combinations.

Best performing vault-section combination	Correct classification rate (%)	Mis-classification rate (%)	Rejection type	Correct classification rate with rejection (%)	Mis-classification rate with rejection (%)	Rejection rate (%)
TV: PCA_{TV} -LDC	95.2%	4.8%	Ambiguity (5%)	91.2%	3.1%	5.7%
NS: D_{NS} -LDC	99.9%	0.1%	Outlier (1%)	98.1%	0.1%	1.8%
TS: D_{TS} -QDC	96.1%	3.9%	Outlier (5%)	91.8%	2.8%	5.4%
NT: $PCA3_{NT}$ -PARZENC	88.9%	11.1%	Ambiguity (1%)	75.7%	2.7%	21.6%

7 Classification Evaluation

In chapter 4, the vaults of the WC 2010 database are segmented into vault-sections. In chapter 5, regions of interest are proposed which represent the motion characteristics of the vaults. Furthermore, the regions of interest are transformed in feature representations (reduced feature sets) by transformation mappings. In chapter 6, we evaluate the reduced feature set - classifier - rejection combinations per vault-section. Based on the discriminative power of the combinations, the PCA_{TV} -LDC-Amb5%, D_{NS} -LDC-Out1%, D_{TS} -QDC-Out5% and $PCA3_{NT}$ -PARZENC-Amb1% combinations were chosen to represent the motion characteristics of the vault-sections best.

In this chapter, the classification problem is expanded from the classification of individual vault-sections to the classification of a complete vault jump. The classification system is validated by the bootstrapping approach in section 7.1. PCA_{TV} -LDC-Amb5%, D_{NS} -LDC-Out1%, D_{TS} -QDC-Out5% and $PCA3_{NT}$ -PARZENC-Amb1% combinations are used to classify the vault-sections. A complete vault is classified by consecutively classifying the vault-sections. The resulting label is checked with the true label provided by the FIG code of points. Section 7.2 concludes the chapter.

7.1 Results Vault Classification

We will first evaluate the classification performance of the combined vault-sections classification system for all test samples. The vaults with label ‘Yurchenko-0somersaults-layout-0twists’ and ‘Tsukahara-1somersault-layout-3twists’ are excluded from the database, because the 0somersaults and 3twists section-classes are not included in the section-classifiers. This leaves 43 different vault classes to be classified. This test gives an estimation of the overall performance of the system for complete vault classification. Furthermore, by examining the misclassifications, we acquire insight into the influence of the individual vault-sections on the performance of the combined vault-section classification. The system is evaluated by bootstrapping. In total 1000 repetitions are made, where for each repetition 10 test samples are randomly drawn. If either of the vault-sections is misclassified, the complete vault is misclassified. Likewise for the rejection label. This implies that the performance of the classification system is at most as good as the performance of the NT vault-section.

In addition to the evaluation of the overall performance of the system, we also evaluate the influence of the segmentation methodology on the classification performance. We do this by comparing the classification performance of the combined vault-section classification with the classification performance of a system that does not segment the vault into vault-sections, from here on referred to as the conventional classification system. The evaluation includes only the 17 classes that contain 10 or more samples as test samples. The evaluation is done by bootstrapping.

7.1.1 Combined Vault-Sections Evaluation

In Table 7.1, the classification results are given for the combined vault-sections classification. The last column of Table 7.1 gives the percentages of the correctly classified test samples (Correct-Classified), wrongly classified test samples (Miss-Classified), rejected samples which would otherwise be correctly classified (Correct-Rejected) and rejected samples which would otherwise be wrongly classified (Miss-Rejected).

Table 7.1 shows that the maximum correct classification rate for classifying complete vault jumps is 80.0%. However, no rejection is applied, resulting in a classification error rate of 20.0%. By applying rejection, 69.5% of the vaults are classified and 30.5% rejected. Of the classified vaults, 90.2% is correctly classified and 9.8% is misclassified. Of the rejected vaults, 56.7% are negative rejections and 43.3% are positive rejections. From the 43 presented vault classes to the system, 35 vault classes are classified (32 classes correctly). However, the 11 vault classes that cannot be correctly classified included only 1 sample in the WC2010 database. It is thought that if a higher number of test samples are presented to the combined system, it is capable of correctly classifying samples from all 43 classes.

Table 7.1 Results complete vault classification, with and without rejection.

System setup	Total classified/rejected (%)	Classified as (%)
Complete Vault Classification. No rejection. <i>PCA_{TV}</i> -LDC <i>D_{NS}</i> -LDC <i>D_{TS}</i> -QDC <i>PCA_{3NT}</i> -PARZENC	100%/0%	Correct-Classified (80.0%)
		Correct-Rejected (0%)
		Miss-Classified (20.0%)
		Miss-Rejected (0%)
Complete Vault Classification. With rejection. <i>PCA_{TV}</i> -LDC-Ambiguity(5%) <i>D_{NS}</i> -LDC-Outlier(1%) <i>D_{TS}</i> -QDC-Outlier(5%) <i>PCA_{3NT}</i> -PARZENC(1%)	69.5%/30.5%	Correct-Classified (62.7%)
		Correct-Rejected (17.3%)
		Miss-Classified (6.8%)
		Miss-Rejected (13.2%)

To gain more knowledge about the weaknesses of the classification system, we investigate the misclassifications of the full vault classification, with and without rejection. The results are given in Table 7.2.

Table 7.2 Contribution of the vault-sections to the misclassification rate. Percentages are for total amount of misclassifications. The true number of misclassified samples is given between brackets.

System setup	Percentage per section/multiple sections						
	TV	NS	TS	NT	TV+TS	TV+NT	TS+NT
No rejection, 20.0% miss (2004 samples)	18.8% (377)	1.1% (23)	15.7% (314)	50.8% (1018)	2.6% (53)	5.7% (115)	5.2% (104)
With rejection, 6.8% miss (618 samples)	30.0% (204)	3.1% (21)	25.0% (170)	36.3% (247)	0.00% (0)	0.00% (0)	5.7% (39)

Table 7.2 shows that for the system without rejection, the majority of the misclassifications is due to the misclassification of the number of twists, as was to be expected from the Vault-section evaluation. Furthermore, 13.5% of the misclassifications are due to the misclassification of multiple sections. When rejection is applied, the 20% misclassification rate of the total amount of samples, is reduced to 6.8% (681 of the 10000 samples misclassified). Table 7.2 shows that the rejection has the most effect on the number of misclassified NT-samples, this is conform the vault-section experiments, which showed the highest number of rejections for the NT vault-section. Furthermore, the rejection rejects all the samples that where misclassified by both TV and TS/NT.

7.1.2 Segmentation Evaluation

For training the combined section-classification, all the samples of the WC2010 database are used, except for the 0 somersaults samples and the 3 twists samples. Note that also the 26 vault classes containing less than 10 samples are used for training. For the training the conventional classification system, only the samples of the 17 test classes are used. For the conventional classification system we used the LDC-ambiguity rejection classifier combined with the PCA transformation mapping applied to all the vault-section regions of interest. The PCA-transformation mapping showed proper results in all vault-section experiments of chapter 6. The LDC-Ambiguity rejection performed best. On average, the PCA mapping is able to cover 99% of the variance by 11 principal components. During training, 5% of the training samples is rejected by the ambiguity rejection.

The combined vault-sections classification system classifies 71.8% of the samples. Of the classified samples, 92.4% is correctly classified and 7.6 % is misclassified. In total, 66.4% of the test samples is correctly classified, 5.4% is misclassified and 28.2% is rejected.

The conventional classification system classifies 94.5% of the samples. Of the classified samples, 74.7% is correctly classified and 25.3% is misclassified. In total, 70.5% of the test samples is correctly classified, 23.9% is misclassified and 5.5% is rejected.

7.2 Conclusion

The segmentation evaluation experiments show that the performance of the combined system exceeds the performance of the conventional system. The combined vault-sections evaluation experiments show that the combined system is not only a more robust system but also a more versatile system.

By the full classification experiments we have gained insight into the performance of the four vault-section classifiers combined to classify a complete jump. The combined vault-sections evaluation experiments show that the combined system has a classification rate of 69.5% with a correct classification accuracy of 90.2%. As was expected from the vault-section experiments, the majority of the rejections and misclassifications are due to the classification of the number of twists.

For the 17 classes that contain more than 10 samples, the combined system has a classification rate of 71.8% with a correct classification accuracy of 92.4%.

8 Conclusion

In this thesis we have investigated the application of automatic classification for vault jumps based on video analysis. The classification is based on the combined classification of four vault-sections; Type of Vault, Number of Somersaults, Type of Somersaults, Number of twists. The automatic vault classification system transforms the video images to feature representations, which reflect the specific characteristics of different vault jumps in the four vault-sections. Then, the four vault-section feature sets are automatically classified using for each vault-section a specific feature set - classifier - rejection combination. Then the complete vault label is determined by the combination of the estimated vault-section labels.

The main contributions of this thesis are as follows. Firstly, we developed a segmentation methodology, which allows for a versatile classification system. By segmenting the classification of a complete vault jump into a sequence of vault-section classifications we are able to use a limited amount of data (618 samples, 45 vault classes) to design a classification system capable of classifying a higher number of vault classes than the number of vault classes included in the training database. Secondly, we systematically analyzed the individual vault-sections on their classification performance. Here, our goal was to find the best performing feature set - classifier - rejection combination for each vault-section. To this end, we introduced multiple feature sets, multiple classifiers and multiple rejection types for each vault-section. We then thoroughly investigated all feature set - classifier - rejection combinations on their discriminative power by which we choose a best combination per vault-section. Thirdly, we have investigated the overall performance of the chosen vault-section classification combinations in classifying a complete vault jump.

By using the techniques presented in this thesis we obtained a complete vault classification rate of 69.5% (90.2% correct, 9.8% misclassified). The experiments conducted in this thesis showed that the Number of Somersaults vault-section has the highest classification performance and accuracy, followed by the Type of Somersault and Type of Vault vault-section. With a classification rate of 78.4% (96.6% correct, 3.4% misclassified) and a rejection rate of 21.6%, the Number of Twists vault-section has the lowest classification performance. This is due to high inner-class variances in the examined feature sets, arising from different twisting-styles and background noise in the video images.

9 Discussion

This chapter contains the discussions of the vault-section evaluation and classification evaluation experiments. This discussion focuses mainly on the classification of the Number of Twists vault-section, which proves to be the weakest vault-section classification. Furthermore, a discussion will be held on the practical implementation of the system in a gymnasium.

The quality of the classification system is directly influenced by the quality of the video images and the quality of the performed vaults. A poorly executed vault is more difficult to classify than a well performed one. A recording is considered of high quality if the entire vault motion, from the preparation phase to the landing, is captured with a low degree of background noise. As stated in section 3.4, the video analysis system “TurnTrainersCockPit” (TTCP), focuses on the dynamical motions of the gymnast performing a vault jump. The majority of the movements on the background are excluded reducing the background noise. However, objects moving in the background that cross paths with the movements of the gymnast in the foreground are not excluded and induce errors. Thus a high degree of background movements results in a low quality video recording.

The bootstrap experiments of the vault-section evaluation show that the Number of Twists vault-section classification, consisting of the $PCA3_{NT}$ -PARZENC-Amb1% combination, produces a classification rate of 78.4% (96.6% correct, 3.4% misclassified) and a rejection rate of 21.6%. If no rejection is applied, 88.9% of the test samples is correctly classified, leaving 11.1% to be misclassified. To gain insight in the misclassifications of the system, we will investigate the confusion matrices of the $PCA3_{NT}$ -PARZENC-Amb1% combination. The confusion matrices, with and without rejection, are given in tables 9.1 and 9.2. The confusion matrix without rejection shows two trends in the misclassifications. Firstly, all classes contain samples that are confused with the 0 Twists class. Secondly, the remaining misclassification lie near the diagonal of the confusion matrix.

As stated in section 5.1, the twist classes are characterized by the number of oscillations included in the normalized observed area and Hu Moment 1 particle measurements of the second flight phase (A_{SFP} , $Hu_{1_{SFP}}$). Furthermore, normalizing the particle measurements to $[-1,1]$ stresses the oscillations. An oscillation results from the transition of the observed body from the sagittal plane, through the coronal plane, back to the sagittal plane. The amplitude of the oscillations in A_{SFP} is determined by the ratio between the observed area in the sagittal plane and the coronal plane. The amplitude of the oscillations in $Hu_{1_{SFP}}$ is determined by the ratio between the observed shape of the body in the sagittal plane and the coronal plane. The high confusion rate with the 0 Twists class, indicates that for some samples the amplitudes are too small to be recognized by the classification system. It is thought that deviations from the layout body posture and gender physiques play a role in the decrease of the amplitudes. For example, the area and shape of the tucked body posture in the sagittal plane does not differ much from the area and the shape in the coronal plane. Also, female gymnasts have a more slender physique in the coronal plane and a broader physique in the sagittal plane, than male gymnasts. Furthermore, female gymnasts often put their hair in a knot or ponytail which increases the observed area in the sagittal plane. These factors decrease the amplitude of the oscillations.

The confusions near the diagonal of the confusion matrix indicate that NT-classes that differ by half a twist are confused. This indicates that some oscillations are obscured and lose their distinctive power. Maintaining a constant layout body posture during twisting results in characteristic distinctive oscillations. Throughout the majority of the second flight phase the body posture is constant. However, just after the moment of last hand contact with the vaulting table and just before the landing, the body posture is not constant. In general, twisting is initiated by tucking in the arms after the last hand contact with the vaulting table. To prepare for landing, the twisting motion is stopped by stretching out the arms. These changes in body posture, obscure the twists made during the initiation and completion of the second flight phase.

By the segmentation of the vault jump into vault-sections and basing the classification of the vault jump on the combined classification of the vault-sections we assumed the vault-sections to be independent. The combined vault-section evaluation experiments, conducted in section 7.1.1, showed no direct relation between the misclassification of one of the vault-sections and the classification performance of the other vault-sections. However, this does not exclude the presence of correlations between the motions performed in the first flight phase and the second flight phase. After all, these are linked. For example, Tsukahara vaults include a $\frac{1}{4}$ twist in the first flight phase, resulting in a sideways push-off from the vaulting table, while the other vault types result in a forward or backward push-off, see the figures in Table 2.1. A gymnast is not allowed to land sideways, thus Tsukahara vaults always include an additional $\frac{1}{4}$ twist in the second flight phase, for example $\frac{3}{4}$ twists is labeled as $\frac{1}{2}$ twist.

The vault classification system of this thesis is based on the recordings of the vault jumps performed at the world championships in gymnastics of 2010. This implies that all the vault jumps are performed by professional gymnasts with a near perfect execution. This increases the discriminative power of the feature sets. Furthermore, the recordings are of high quality with a low amount of background movements.

For a one-to-one implementation of the classification system developed in this thesis in a gymnasium, the setup of the TTCP system in the gymnasium is required to be identical to the setup of the world championships. This implies that the video images made in the gymnasium are of equal quality as the world championships, thus have a low degree of background noise, but most of all have an equal capturing volume.

In general, the recordings made in a gymnasium are of a lower quality than the recordings of the world championships. The amount of background motions in a gymnasium is generally higher and the capturing volume of the video cameras often differs from that of the world championships setup, thus a direct implementation of the developed classification system would result in unreliable classifications. The design methods used in this thesis can serve as guidance in modifying the classification system to the TTCP setup in the gymnasium. This includes regenerating the feature sets and retraining the classifiers.

Table 9.1 Confusion matrix of $PCA3_{NT}$ -PARZENC, based on TST.

True class labels	Estimated class labels (tw=twists)						Total	
	0 tw	0.5 tw	1 tw	1.5 tw	2 tw	2.5 tw	True:	Correct:
0 twists	62	2	1	0	0	0	65	95.4%
0.5 twists	3	22	0	0	0	0	25	88.0%
1 twists	6	2	55	4	0	0	67	82.1%
1.5 twists	1	0	0	26	2	2	31	83.9%
2 twists	3	1	0	0	67	8	79	84.8%
2.5 twists	3	0	0	0	2	31	36	86.1%
Total:	78	27	56	30	71	41	303	86.7%

Table 9.2 Confusion matrix of $PCA3_{NT}$ -PARZENC-Amb1%, based on TST.

True class labels	Estimated class labels (tw=twists)							Total	
	0 tw	0.5 tw	1 tw	1.5 tw	2 tw	2.5 tw	Rejected	True:	Correct:
0 twists	38	1	0	0	0	0	26	65	97.4%
0.5 twists	1	13	0	0	0	0	11	25	92.6%
1 twists	1	0	32	0	0	0	34	67	97.0%
1.5 twists	1	0	0	14	1	0	15	31	87.5%
2 twists	0	0	0	0	47	1	31	79	97.9%
2.5 twists	0	0	0	0	0	22	14	36	100%
No label	0	0	0	0	0	0	0	0	-
Total:	41	14	32	14	48	23	131	303	95.4%

10 Recommendations

The classification system developed in this thesis proves the concept of automatically classifying vault jumps based on video analysis. However, there is room for improvement.

To improve the robustness of the classification system, we recommend to include more training data to ensure that all the vault-section classes are represented by an sufficient equal amount of training samples. To improve the completeness of the classification system, we recommend to expand the classification system with the 0 somersaults NS-class, 3 twists NT-class and the Yurchenko 1/1 TV-class. By this the classification system should be able to classify all the 104 vault-classes from the FIG Code of Points.

The experiments conducted in this thesis show that the most room for improvement lies in the classification of the Number of Twists vault-section. While the observed area and the Hu Moment 1 particle measurements prove to contain the highest discriminative power of all particle measurements included in this thesis, the discussion held in chapter 9, implies that the discriminative power is not high enough. Furthermore, the particle measurements are too sensitive to background noise. This results in a low correct classification rate.

By expanding the capturing volume of the TTCP system with an additional camera, which records the vault motions in a front view, a 3-D capturing volume is obtained. It is thought, that by relating the video images of the two cameras to each other, more distinctive particle measurements can be computed. Front view recordings not only provide more information about the motion characteristics of a vault jump, they also provide information about the observed background noise in side view recordings. It is expected that the background motions observed by one camera are not observed by the other camera, thus a correction can be made for the background noise. However, the correction cannot be made if one of the cameras observes a background motion and at the same time the other camera observes a different background motion. This will still induce errors.

Relating the particle measurements of two camera's to each other to distinguish specific vault characteristics is expected to be a challenging task. One of the challenges to be overcome is the fact that some particle measurements of front view recordings are influenced by multiple vault-sections. For example, the area and Hu moment 1 particle measurements of front view recordings are not only influenced by the body posture and twisting motions, but also by somersault motions and flight trajectory. It is thought that by including the x-CoM, y-CoM and orientation particle measurements of side view recordings in the relation between the observed area of front and side view recordings and the relation between the Hu moment 1 particle measurements of front and side view recordings, a correction can be made for the influence of somersaults and flight trajectory on the observed area and Hu moment 1 particle measurements of front view recordings.

To summarize; we believe that expanding the capturing volume with a front view camera allows for more distinctive feature sets and a better classification performance. However, generating these feature sets will prove to be a challenging task.

Acknowledgements

I would like to thank a number of people who assisted me during my thesis. Firstly, I would like to thank my supervisor Prf. dr. H.E.J. Veeger, whose advice and support contributed essentially to the outcome of my study. Secondly, I would like to give special thanks to dr. ir. J.W. van der Eb of the VU Amsterdam, for collecting and submitting the recordings database. Without these recordings, I would have not been able to create the proposed classification system. Furthermore, his expertise and support added considerably to the design of the classification system. Thirdly, I would like to thank dr. D.M.J. Tax of the Pattern recognition and Bioinformatics department of the TU Delft, for providing the knowledge needed to design the classification principle. Furthermore, I would like to thank the Pattern Recognition Laboratory research group of the TU Delft Faculty of Electrical Engineering, Mathematics and Computer sciences for submitting the PRTools Matlab toolbox. Fourthly, I would like to thank Drs. M.J.J.J. Aarts, manager InnoSportLab `s-Hertogenbosch, for his contribution in setting up the project.

Finally, I would like to thank my friends, girlfriend and parents for supporting me during my whole research.

Appendix A

A.1 TV-50-50 Split Experiment Results

In this appendix the results of the best performing classifier - rejection combinations per reduced feature set are given for the 50-50 split experiments for the Type of Vault (TV) vault-section. The results are given in Table A.1.1, which is partitioned as follows. The first two columns indicate the reduced feature set - classifier combination. The third column gives the classification error estimate without rejection. The fourth column gives the total number of misclassifications. The fifth column indicates which rejection type is used. The sixth column gives the total number of misclassifications with rejection. The last column gives the number of rejected samples. In addition to Table A.1.1, the confusion matrices of the best performing (highlighted) classifier - rejection combinations per feature set are given in tables A.1.2 to A.1.7. The confusion matrices are based on the test samples of the TV-50-50 split experiments (TV-TST). The percentages given in the last column of the confusion matrices, indicate the true correct classification rate per class.

Table A.1.1 TV-50-50 experiment results for the Type of Vault vault-section (over 303 test samples).

Reduced feature set	Classifier	Classification error estimate (%)	Total misses	Rejection type (5%)	Total misses with rejection	Rejected
Delta Feature (D_{TV})	LDC	7.3%	28	Outlier	24	13
	LOGLC	8.0%	23	Ambiguity	16	19
	QDC	7.3%	28	Outlier	23	13
	PARZENDC	7.1%	27	Ambiguity	16	23
Principal Component Analysis (PCA_{TV})	NMC	7.0%	22	Ambiguity	16	15
	LDC	5.1%	17	Ambiguity	8	23
	SVC	9.0%	19	Ambiguity	15	24
	PARZENC	4.8%	16	Ambiguity	6	49
	PARZENDC	7.5%	25	Ambiguity	4	56
Dynamic Time Warping (DTW)	Temp1_{TV}	5.3%	17	Ambiguity*	11	11
	Temp2 _{TV}	7.5%	22	Ambiguity*	17	9

*DTW rejection is based on 5% difference between the lowest two costs, not 5% of the TRN data.

Table A.1.2 Confusion matrix of D_{TV} -LOGLC, based on TV-TST.

True class labels	Estimated class labels				Total	
	Handspring	Tsukahara	Yurchenko	Yurchenko ½	True:	Correct:
Handspring	60	6	1	0	67	89.6%
Tsukahara	11	104	0	0	115	90.4%
Yurchenko	0	0	105	4	109	96.3%
Yurchenko ½	0	0	1	11	12	91.7%
Total:	71	110	107	15	303	92.0%

Table A.1.3 Confusion matrix of D_{TV} - LOGLC-Ambiguity, based on TV-TST.

True class labels	Estimated class labels					Total	
	Handspring	Tsukahara	Yurchenko	Yurchenko $\frac{1}{2}$	Rejected	True:	Correct:
Handspring	55	4	1	0	7	67	82.1%
Tsukahara	7	97	0	0	11	115	84.3%
Yurchenko	0	0	105	3	1	109	96.3%
Yurchenko $\frac{1}{2}$	0	0	1	11	0	12	91.7%
No label	0	0	0	0	0	0	-
Total:	62	101	107	14	19	303	88.8%

Table A.1.4 Confusion matrix of PCA_{TV} -LDC, based on TV-TST.

True class labels	Estimated class labels				Total	
	Handspring	Tsukahara	Yurchenko	Yurchenko $\frac{1}{2}$	True:	Correct:
Handspring	58	8	1	0	67	86.6%
Tsukahara	4	110	0	1	115	95.7%
Yurchenko	1	1	106	1	109	97.2%
Yurchenko $\frac{1}{2}$	0	0	0	12	12	100%
Total:	63	119	107	14	303	94.9%

Table A.1.5 Confusion matrix of PCA_{TV} -LDC-Ambiguity, based on TV-TST.

True class labels	Estimated class labels					Total	
	Handspring	Tsukahara	Yurchenko	Yurchenko $\frac{1}{2}$	Rejected	True:	Correct:
Handspring	56	4	1	0	6	67	83.6%
Tsukahara	0	100	0	1	14	115	87.0%
Yurchenko	1	1	105	0	2	109	96.3%
Yurchenko $\frac{1}{2}$	0	0	0	11	1	12	91.7%
No label	0	0	0	0	0	0	-
Total:	57	105	106	12	23	303	89.7%

Table A.1.6 Confusion matrix of $DTW-Temp1_{TV}$, based on TV-TST.

True class labels	Estimated class labels				Total	
	Handspring	Tsukahara	Yurchenko	Yurchenko $\frac{1}{2}$	True:	Correct:
Handspring	57	6	3	1	67	85.1%
Tsukahara	1	114	0	0	115	99.1%
Yurchenko	4	1	103	1	109	94.5%
Yurchenko $\frac{1}{2}$	0	0	0	12	12	100%
Total:	65	115	106	14	303	94.7%

Table A.1.7 Confusion matrix of *DTW-Temp1_{TV}* with rejection (diff>5%), based on TV-TST.

True class labels	Estimated class labels					Total	
	Handspring	Tsukahara	Yurchenko	Yurchenko $\frac{1}{2}$	Rejected	True:	Correct:
Handspring	55	6	1	0	5	67	73.1%
Tsukahara	1	113	0	0	1	115	93.9%
Yurchenko	3	0	102	0	4	109	92.7%
Yurchenko $\frac{1}{2}$	0	0	0	11	1	12	91.7%
No label	0	0	0	0	0	0	-
Total:	59	119	103	11	11	303	87.9%

A.2 NS-50-50 Split Experiment Results

In this appendix the results of the best performing classifier - rejection combinations per reduced feature set are given for the 50-50 split experiments for the Number of Somersaults (NS) vault-section. The results are given in Table A.2.1, which is partitioned as follows. The first two columns indicate the reduced feature set - classifier combination. The third column gives the classification error estimate without rejection. The fourth column gives the total number of misclassifications. The fifth column indicates which rejection type is used. The sixth column gives the total number of misclassifications with rejection. The last column gives the number of rejected samples. In all combinations, the single misclassification consisted of a confusion between a sample of the 1 somersaults class with the 2 somersaults class.

Table A.2.1 NS-50-50 split experiment results for the Number of Somersaults vault-section (over 303 test samples).

Reduced feature set	Classifier	Classification error estimate (%)	Total misses	Rejection type (5%)	Total misses with rejection	Rejected
Delta Feature (D_{NS})	LDC	0.18%	1	Outlier	0	23
	PARZENC	0.18%	1	Outlier	0	27
	QDC	0.18%	1	Outlier	1	22
	PARZENDC	0.18%	1	Outlier	0	41
Principal Component Analysis (PCA_{NS})	LDC	0.18%	1	Outlier	0	18
	PARZENC	0.18%	1	Outlier	0	18
	PARZENDC	0.18%	1	Outlier	0	11
	BPXNC	0.18%	1	Outlier	1	23

A.3 TS-50-50 Split Experiment Results

In this appendix the results of the best performing classifier - rejection combinations per reduced feature set are given for the 50-50 split experiments for the Type of Somersault (TS) vault-section. The results are given in Table A.3.1, which is partitioned as follows. The first two columns indicate the reduced feature set - classifier combination. The third column gives the classification error estimate without rejection. The fourth column gives the total number of misclassifications. The fifth column indicates which rejection type is used. The sixth column gives the total number of misclassifications with rejection. The last column gives the number of rejected samples. In addition to Table A.3.1, the confusion matrices of the best performing (highlighted) classifier - rejection combinations per feature set are given in tables A.3.2 to A.3.9. The confusion matrices are based on the test samples of the TS-50-50 split experiments (TS-TST). The percentages given in the last column of the confusion matrices, indicate the true correct classification rates per class.

Table A.3.1 TS-50-50 split experiment results for the Type of Somersaults vault-section (over 303 test samples).

Reduced feature set	Classifier	Classification error estimate (%)	Total misses	Rejection type (5%)	Total misses with rejection	Rejected
Delta Feature (D_{TS})	LDC	8.0%	17	Outlier	12	12
	LOGLC	8.4%	15	Outlier	11	14
	QDC	6.7%	16	Outlier	10	17
	PARZENDC	7.3%	14	Ambiguity	6	22
Principal Component Analysis (PCA_{TS})	LDC	8.3%	23	Outlier	20	8
	PARZENC	11.8%	16	Ambiguity	1	47
	KNNC	13.4%	16	Ambiguity	14	2
	QDC	21.1%	24	Outlier	9	45

Table A.3.2 Confusion matrix of D_{TS} -QDC, based on TST.

True class labels	Estimated class labels			Total	
	Layout	Piked	Tucked	True:	Correct:
Layout	219	9	1	229	95.6%
Piked	1	32	1	34	94.1%
Tucked	1	3	36	40	90.0%
Total:	221	44	38	303	93.2%

Table A.3.3 Confusion matrix of D_{TS} -QDC-Outlier , based on TS-TST.

True class labels	Estimated class labels				Total	
	Layout	Piked	Tucked	Rejected	True:	Correct:
Layout	209	5	1	14	229	91.3%
Piked	0	31	1	2	34	91.2%
Tucked	1	2	36	1	40	90.0%
No label	0	0	0	0	0	-
Total:	210	38	38	17	303	90.8%

Table A.3.4 Confusion matrix of D_{TS} -PARZENDC, based on TS-TST.

True class labels	Estimated class labels			Total	
	Layout	Piked	Tucked	True:	Correct:
Layout	222	6	1	229	96.9%
Piked	1	31	2	34	91.2%
Tucked	1	3	36	40	90.0%
Total:	224	40	39	303	92.7%

Table A.3.5 Confusion matrix of D_{TS} -PARZENDC-Ambiguity, based on TS-TST.

True class labels	Estimated class labels				Total	
	Layout	Piked	Tucked	Rejected	True:	Correct:
Layout	138	2	0	44	229	60.1%
Piked	0	10	1	23	34	29.4%
Tucked	0	1	24	15	40	60.0%
No label	0	0	0	0	0	-
Total:	183	13	25	82	303	49.8%

Table A.3.6 Confusion matrix of PCA_{TS} -PARZENC, based on TS-TST.

True class labels	Estimated class labels			Total	
	Layout	Piked	Tucked	True:	Correct:
Layout	225	3	1	229	98.3%
Piked	3	26	5	34	76.5%
Tucked	2	2	36	40	90.0%
Total:	230	31	42	303	88.3%

Table A.3.7 Confusion matrix of PCA_{TS} -PARZENC-Ambiguity , based on TS-TST.

True class labels	Estimated class labels				Total	
	Layout	Piked	Tucked	Rejected	True:	Correct:
Layout	205	1	0	23	229	89.5%
Piked	0	19	0	15	34	55.9%
Tucked	0	0	31	9	40	77.5%
No label	0	0	0	0	0	-
Total:	205	20	31	47	303	74.3%

Table A.3.8 Confusion matrix of PCA_{TS} -KNNC, based on TS-TST.

True class labels	Estimated class labels			Total	
	Layout	Piked	Tucked	True:	Correct:
Layout	227	1	1	229	99.1%
Piked	5	24	5	34	70.6%
Tucked	2	2	36	40	90.0%
Total:	234	27	42	303	86.6%

Table A.3.9 Confusion matrix of PCA_{TS} -KNNC-Ambiguity, based on TS-TST.

True class labels	Estimated class labels				Total	
	Layout	Piked	Tucked	Rejected	True:	Correct:
Layout	227	1	1	0	229	99.1%
Piked	3	24	5	2	34	70.6%
Tucked	2	2	36	0	40	90.0%
No label	0	0	0	0	0	-
Total:	210	38	38	17	303	86.6%

A.4 NT-50-50 Split Experiment Results

In this appendix the results of the best performing classifier - rejection combinations per reduced feature set are given for the 50-50 split experiments for the Number of Twists (NT) vault-section. The results are given in Table A.4.1, which is partitioned as follows. The first two columns indicate the reduced feature set - classifier combination. The third column gives the classification error estimate without rejection. The fourth column gives the total number of misclassifications. The fifth column indicates which rejection type is used. The sixth column gives the total number of misclassifications with rejection. The last column gives the number of rejected samples. In addition to Table A.4.1, the confusion matrices of the best performing (highlighted) classifier - rejection combinations per feature set are given in tables A.4.2 to A.4.9. The confusion matrices are based on the test samples of the NT-50-50 split experiments (NT-TST). The percentages given in the last column of the confusion matrices, indicate the true correct classification rates per class.

Table A.4.1 NT-50-50 split experiment results for the Number of Twists vault-section (over 303 test samples).

Reduced feature set	Classifier	Classification error estimate(%)	Total misses	Rejection type	Total misses with rejection (5%)	Rejected
Principal Component Analysis A_{SFP} ($PCA1_{NT}$)	PARZENC	21.8%	65	Ambiguity	33	64
	KNNC	20.3%	55	Ambiguity	0	303
	QDC	33.9%	82	Outlier	54	77
	PARZENDC	29.9%	91	Ambiguity	39	89
Principal Component Analysis Hu_{1SFP} ($PCA2_{NT}$)	PARZENC	24.3%	61	Ambiguity	30	61
	KNNC	24.7%	61	Ambiguity	0	303
	QDC	37.1%	85	Outlier	53	75
	PARZENDC	30.6%	75	Ambiguity	47	49
Principal Component Analysis $[A_{SFP}, Hu_{1SFP}]$ ($PCA2_{NT}$)	FISHERC	32.4%	80	Ambiguity	71	13
	PARZENC	13.3%	40	Ambiguity(5%)	6	131
				Ambiguity(1%)	13	63
	KNNC	14.9%	39	Ambiguity	0	303
	PARZENDC	24.5%	67	Ambiguity	8	194
Dynamic Time Warping (DTW)	$Temp1_{NT}$	28.0%	74	Ambiguity*	50	40
	$Temp2_{NT}$	23.2%	67	Ambiguity*	36	54

*DTW rejection is based on 5% difference between the lowest two costs, not 5% of the TRN data.

Table A.4.2 Confusion matrix of $PCA1_{NT}$ -PARZENC, based on NT-TST.

True class labels	Estimated class labels (tw=twists)						Total	
	0 tw	0.5 tw	1 tw	1.5 tw	2 tw	2.5 tw	True:	Correct:
0 twists	58	3	3	1	0	0	65	89.3%
0.5 twists	3	21	1	0	0	0	25	84.0%
1 twists	13	3	48	3	0	0	67	71.6%
1.5 twists	4	2	2	19	3	1	31	61.3%
2 twists	7	2	0	2	61	7	79	77.2%
2.5 twists	3	0	0	0	2	31	36	86.1%
Total:	88	31	54	25	66	39	303	78.3%

Table A.4.3 Confusion matrix of $PCA1_{NT}$ -PARZENC-Ambiguity, based on NT-TST.

True class labels	Estimated class labels (tw=twists)							Total	
	0 tw	0.5 tw	1 tw	1.5 tw	2 tw	2.5 tw	Rejected	True:	Correct:
0 twists	52	2	2	0	0	0	9	65	80.0%
0.5 twists	2	19	1	0	0	0	3	25	76.0%
1 twists	5	3	39	1	0	0	19	67	58.2%
1.5 twists	1	1	2	17	2	0	8	31	54.8%
2 twists	2	2	0	0	50	5	20	79	63.3%
2.5 twists	1	0	0	0	1	29	5	36	80.6%
No label	0	0	0	0	0	0	0	0	-
Total:	63	27	44	18	53	34	64	303	68.8%

Table A.4.4 Confusion matrix of $PCA2_{NT}$ -PARZENC, based on NT-TST.

True class labels	Estimated class labels (tw=twists)						Total	
	0 tw	0.5 tw	1 tw	1.5 tw	2 tw	2.5 tw	True:	Correct:
0 twists	52	9	2	2	0	0	65	80.0%
0.5 twists	13	12	0	0	0	0	25	60.0%
1 twists	3	3	57	3	0	0	67	85.1%
1.5 twists	5	1	1	21	1	2	31	67.7%
2 twists	3	0	1	2	69	4	79	87.3%
2.5 twists	3	0	0	0	2	31	36	86.1%
Total:	79	25	61	28	72	38	303	77.7%

Table A.4.5 Confusion matrix of $PCA2_{NT}$ -PARZENC-Ambiguity, based on NT-TST.

True class labels	Estimated class labels (tw=twists)							Total	
	0 tw	0.5 tw	1 tw	1.5 tw	2 tw	2.5 tw	Rejected	True:	Correct:
0 twists	43	5	1	0	0	0	16	65	66.2%
0.5 twists	6	8	0	0	0	0	11	25	32.0%
1 twists	2	3	50	2	0	0	10	67	74.6%
1.5 twists	1	0	0	17	0	1	12	31	54.8%
2 twists	0	0	1	1	66	3	8	79	83.5%
2.5 twists	2	0	0	0	2	28	4	36	77.8%
No label	0	0	0	0	0	0	0	0	-
Total:	54	16	52	20	68	32	61	303	64.8%

Table A.4.6 Confusion matrix of $PCA3_{NT}$ -PARZENC, based on NT-TST.

True class labels	Estimated class labels (tw=twists)						Total	
	0 tw	0.5 tw	1 tw	1.5 tw	2 tw	2.5 tw	True:	Correct:
0 twists	62	2	1	0	0	0	65	95.4%
0.5 twists	3	22	0	0	0	0	25	88.0%
1 twists	6	2	55	4	0	0	67	82.1%
1.5 twists	1	0	0	26	2	2	31	83.9%
2 twists	3	1	0	0	67	8	79	84.8%
2.5 twists	3	0	0	0	2	31	36	86.1%
Total:	78	27	56	30	71	41	303	86.7%

Table A.4.7 Confusion matrix of $PCA3_{NT}$ -PARZENC-Ambiguity, based on NT-TST.

True class labels	Estimated class labels (tw=twists)							Total	
	0 tw	0.5 tw	1 tw	1.5 tw	2 tw	2.5 tw	Rejected	True:	Correct:
0 twists	38	1	0	0	0	0	26	65	58.5%
0.5 twists	1	13	0	0	0	0	11	25	52.0%
1 twists	1	0	32	0	0	0	34	67	47.8%
1.5 twists	1	0	0	14	1	0	15	31	45.2%
2 twists	0	0	0	0	47	1	31	79	59.5%
2.5 twists	0	0	0	0	0	22	14	36	61.1%
No label	0	0	0	0	0	0	0	0	-
Total:	41	14	32	14	48	23	131	303	54.0%

Table A.4.8 Confusion matrix of $DTW-Temp2_{NT}$, based on NT-TST.

True class labels	Estimated class labels (tw=twists)						Total	
	0 tw	0.5 tw	1 tw	1.5 tw	2 tw	2.5 tw	True:	Correct:
0 twists	43	9	1	1	0	0	65	66.2%
0.5 twists	8	13	1	3	0	0	25	52%
1 twists	1	4	55	5	2	0	67	82.1%
1.5 twists	0	0	1	26	1	3	31	83.9%
2 twists	0	0	0	8	65	6	79	82.3%
2.5 twists	0	0	0	1	1	34	36	94.4%
Total:	52	28	66	44	70	43	303	76.8%

Table A.4.9 Confusion matrix of $DTW-Temp2_{NT}$ with rejection (diff>5%), based on NT-TST.

True class labels	Estimated class labels (tw=twists)							Total	
	0 tw	0.5 tw	1 tw	1.5 tw	2 tw	2.5 tw	Rejected	True:	Correct:
0 twists	41	8	8	0	0	0	8	65	63.1%
0.5 twists	8	10	1	1	0	0	5	25	40%
1 twists	1	3	50	4	1	0	8	67	74.6%
1.5 twists	0	0	1	21	0	3	8	31	67.7%
2 twists	0	0	0	7	59	6	7	79	74.7%
2.5 twists	0	0	0	1	1	32	2	36	88.9%
No label	0	0	0	0	0	0	0	0	-
Total:	50	21	60	34	61	41	36	303	68.2%

Bibliography

- [1] J. Van de Eb, M. Filius, G. Rougoor, C. Van Niel, J. de Water, B. Coolen, and H. de Koning, "Optimal velocity profiles for vault," in *30th Annual Conference of Biomechanics in Sports*, vol. 30, (Melbourne, Australia), pp. 71-75, 2012.
- [2] T. Helten, H. Brock, M. Müller, and H. P. Scheidel, "Classification of trampoline jumps using inertial sensors," *Sports Engineering*, vol. 14, no. 2-4, pp. 155-164, 2011.
- [3] J.P. Foster, M. S. Nixon, and A. Prügel-Bennett, "Automatic gait recognition using area based metrics," *Pattern Recognition Letters*, vol. 24, no. 14, pp. 2489-2497, 2003.
- [4] K. Altun, B. Barshan, and O. Tunçel, "Comparative study on classifying human activities with miniature inertial and magnetic sensors," *Pattern Recognition*, vol. 43, no. 10, pp. 3605-3620, 2010.
- [5] N. F. Troje, "Decomposing biological motion: A framework for analysis and synthesis of human gait patterns," *Journal of Vision*, vol. 2, pp. 371-387, 2002.
- [6] D. Lu and Q. Weng, "A survey of image classification methods and techniques for improving classification performance," *International Journal of Remote Sensing*, vol. 28, no. 5, pp. 823-870, 2007.
- [7] R. Caruana and A. Niculescu-Mizil, "An empirical comparison of supervised learning algorithms," in *International conference on Machine learning*, vol. 23, (New York), pp. 161-168, 2006.
- [8] R. Caruana, N. Karampatziakis, and A. Yessenalina, "An empirical evaluation of supervised learning in high dimensions," in *International Conference on Machine Learning*, vol. 25, (Helsinki, Finland), pp. 96-103, 2008.
- [9] S. Theodoridis and K. Koutroumbas, *Pattern Recognition*. Elsevier, 4th ed., 2009.
- [10] FÉDÉRATION INTERNATIONALE DE GYMNASTIQUE, "Artistic gymnastics history," Retrieved November, 2012, <http://www.fig-gymnastics.com/vsite/vcontent/page/custom/0,8510,5187-188424-205646-44680-282887-custom-item,00.html>.
- [11] C. Frohlich, "Physics of somersaults and twists," *Scientific American*, vol. 242, no. 3, pp. 154-164, 1980.
- [12] FÉDÉRATION INTERNATIONALE DE GYMNASTIQUE, "2013-2016 code of points men's artistic gymnastics," 2012.
- [13] E. J. Sprigings and M. R. Yeadon, "An insight into the reversal of rotation in the hecht vault," *Human Movement Science*, vol. 16, no. 4, pp. 517-532, 1997.
- [14] FÉDÉRATION INTERNATIONALE DE GYMNASTIQUE, "2013-2016 code of points women's artistic gymnastics," 2012.

- [15] L. Wang, T. Tan, H. Ning, and W. Hu, "Silhouette analysis-based gait recognition for human identification," *IEEE Transactions on Pattern Analysis and Machine Intelligence*, vol. 25, no. 12, pp. 1505-1518, 2003.
- [16] T. B. Moeslund, A. Hilton, and V. Krüger, "A survey of advances in vision-based human motion capture and analysis," *Computer Vision and Image Understanding*, vol. 104, no. 2-3, pp. 90-126, 2006.
- [17] H. Brock, M. Müller, and A. Effenber, *Automated Classification of Trampoline Motions Based on Inertial Sensor Input.*, Master's thesis, Saarland University, 2010.
- [18] NATIONAL INSTRUMENTS, "IMAQ vision concepts manual," 2005.
- [19] Matlab PRtools Toolbox, available at <http://www.37steps.com>.
- [20] M. Müller and T. Röder, "Motion templates for automatic classification and retrieval of motion capture data," in *Proceedings of the 2006 ACM SIGGRAPH/Eurographics Symposium on Computer Animation*, ACM Press, pp. 137-146, 2006.